Electrogenic Na/HCO_3 Cotransporter (NBCe1) Variants Expressed in *Xenopus* Oocytes: Functional Comparison and Roles of the Amino and Carboxy Termini

Suzanne D. McAlear, Xiaofen Liu, Jennifer B. Williams, Carmel M. McNicholas-Bevensee, and Mark O. Bevensee

Department of Physiology and Biophysics, University of Alabama at Birmingham, Birmingham, AL 35294

Using pH- and voltage-sensitive microelectrodes, as well as the two-electrode voltage-clamp and macropatch techniques, we compared the functional properties of the three NBCe1 variants (NBCe1-A, -B, and -C) with different amino and/or carboxy termini expressed in *Xenopus laevis* oocytes. Oocytes expressing rat brain NBCe1-B and exposed to a CO_2/HCO_3^- solution displayed all the hallmarks of an electrogenic Na^+/HCO_3^- cotransporter: (a) a DIDS-sensitive pH_i recovery following the initial CO_2-induced acidification, (b) an instantaneous hyperpolarization, and (c) an instantaneous Na^+-dependent outward current under voltage-clamp conditions (−60 mV). All three variants had similar external HCO_3^- dependencies (apparent K_M of 4–6 mM) and external Na^+ dependencies (apparent K_M of 21–36 mM), as well as similar voltage dependencies. However, voltage-clamped oocytes (−60 mV) expressing NBCe1-A exhibited peak HCO_3^--stimulated NBC currents that were 4.3-fold larger than the currents seen in oocytes expressing the most dissimilar C variant. Larger NBCe1-A currents were also observed in current–voltage relationships. Plasma membrane expression levels as assessed by single oocyte chemiluminescence with hemagglutinin-tagged NBCs were similar for the three variants. In whole-cell experiments (V_m = −60 mV), removing the unique amino terminus of NBCe1-A reduced the mean HCO_3^--induced NBC current 55%, whereas removing the different amino terminus of NBCe1-C increased the mean NBC current 2.7-fold. A similar pattern was observed in macropatch experiments. Thus, the unique amino terminus of NBCe1-A stimulates transporter activity, whereas the different amino terminus of the B and C variants inhibits activity. One or more cytosolic factors may also contribute to NBCe1 activity based on discrepancies between macropatch and whole-cell currents. While the amino termini influence transporter function, the carboxy termini influence plasma membrane expression. Removing the entire cytosolic carboxy terminus of NBCe1-C, or the different carboxy terminus of the A/B variants, causes a loss of NBC activity due to low expression at the plasma membrane.

The Journal of General Physiology

INTRODUCTION

Na/HCO_3 cotransporters (NBCs) are functionally diverse proteins that are involved in the regulation of intracellular pH (pH_i), absorption or secretion of HCO_3^-, and maintenance of ion homeostasis in many tissues. The first Na^+/HCO_3^- cotransporter was identified by function in the proximal tubule of the kidney (Boron and Boulpaep, 1983), where the transporter has a 1:3 Na^+:HCO_3^- stoichiometry (Soleimani et al., 1987) and is responsible for reabsorbing as much as ∼90% of filtered bicarbonate (Boron et al., 1997). In glial cells of the central nervous system, an electrogenic Na^+/HCO_3^- cotransporter with a 1:2 Na^+:HCO_3^- stoichiometry (Deitmer and Schlue, 1989; O'Connor et al., 1994; Bevensee et al., 1997a,b) contributes to intracellular and extracellular pH changes that can influence neuronal activity (Chesler, 2003; McAlear and Bevensee, 2004).

At the molecular level, the first cDNA encoding an electrogenic NBC was identified by expression from salamander kidney (Romero et al., 1997). The cloning of salamander kidney NBC paved the way for homology cloning of both electrogenic and electroneutral NBCs, as well as other cation-coupled anion transporters (for review see Romero et al., 2004). Cation-coupled anion transporters in conjunction with anion exchangers (AEs) are members of a superfamily of bicarbonate transporters (BTs). Using the convention introduced by Choi et al. (2000) and expanded by Romero et al. (2004), we refer to the first cloned NBC as NBCe1-A, where "e" refers to electrogenic, "1" refers to the first gene cloned of this family, and "A" refers to the first splice variant identified. The putative membrane topology of NBCe1 shown in Fig. 1 is based on sequence alignment of NBCe1 and AE1 (Romero et al., 1998b). We mapped the NBCe1 sequence on a topology model

S.D. McAlear and X. Liu contributed equally to this work.

Correspondence to Mark O. Bevensee: bevensee@physiology.uab.edu

Abbreviations used in this paper: AE, anion exchanger; DIDS, 4,4′-diisothiocyanatostilbene-2,2′ disulfonate; HA, hemagglutinin; HRP, horseradish peroxidase; NBC, Na/bicarbonate cotransporter; pH_i, intracellular pH; PIP_2, phosphatidylinositol 4,5-bisphosphate; SOC, single-oocyte chemiluminescence.

of the related bicarbonate transporter anion exchanger 1 or AE1 (Taylor et al., 2001). As described by Taylor et al. (2001), the putative topology of AE1 is determined from proteolysis and cysteine accessibility data.

NBCe1 proteins arise from different splice variants of gene *SLC4A4* (Abuladze et al., 2000). The electrogenic Na/HCO_3 cotransporters can be categorized into one of three groups based on differences at the amino and/or carboxy termini (Fig. 1): NBCe1-A ("kidney" clone), NBCe1-B ("heart," "pancreas," and rat-brain 1 NBC clone), and NBCe1-C (rat-brain 2 NBC clone). At the amino acid level, NBCe1-B is identical to NBCe1-A except at the amino terminus where 85 residues replace the 41 residues of NBCe1-A. NBCe1-C is identical to NBCe1-B except at the carboxy terminus where 61 residues replace the 46 residues of NBCe1-B. As reported for the A and B clones from human (Choi et al., 1999), the unique amino terminus of the rat A variant is only 6% identical and 13% homologous to that of the rat B and C variants. Furthermore, while both termini are hydrophilic, ~50% of the 85 amino-terminal residues of the B and C variants are charged residues in contrast to only ~22% of the 41 unique amino-terminal residues of the A variant. Although NBCe1-C has only been reported from rat brain, exon excision between introns at positions 23 and 24 in human *SLC4A4* (Abuladze et al., 2000) would create the unique carboxy terminus. Indeed, using RT-PCR techniques, we have recently identified the full-length cDNAs encoding both NBCe1-B and NBCe1-C from human brain (unpublished data).

Although the physiological significance of the three NBCe1 variants with different amino and/or carboxy termini is not fully known, several investigators have identified specific residues/regions within the cytoplasmic amino and carboxy termini of NBCe1 that contribute to protein function, regulation, and expression. For example, in Ussing-chamber experiments on transfected mouse renal proximal tubule cells, Gross et al. reported that PKA-dependent phosphorylation of the Ser at position 982 within the cytoplasmic carboxy terminus of the A variant (Gross et al., 2001), or position 1026 of the B variant (Gross et al., 2003), changes transporter stoichiometry from 1:3 to 1:2 Na^+:HCO_3^-. This Ser within the cytoplasmic carboxy terminus is common in all three variants. As proposed by the authors, the phosphorylation of the carboxy terminus may induce a conformation change that blocks a HCO_3^- binding site on the transporter. The stoichiometry of the A and B variants appears to be cell type dependent, and not due to the different amino termini (Gross et al., 2001). On the other hand, the amino terminus does contribute to the regulation of transporter activity. For example, Gross et al. (2003) report that the Thr at position 49 of human NBCe1-B is required for the cAMP-stimulated increase in transporter activity. This increase does not appear to involve a change in the phosphorylation of the Thr. Curiously, this Thr is one of two residues that are different in the homologous amino-terminal region of rat NBCe1-B and -C. The carboxy terminus of NBCe1 can also influence expression of the protein. For instance, removing the carboxy-terminal 23 residues of NBCe1-A causes a mistargeting of the transporter to the apical instead of the basolateral membrane when transfected into kidney epithelial cells (Li et al., 2004).

In addition to structure–function data, there is also genetic information that highlights the importance of the cytosolic amino terminus of NBCe1 before the first predicted transmembrane domain. There are human patients with mutations in *SLC4A4* who present primarily with proximal renal tubular acidosis (pRTA) and ocular abnormalities (Igarashi et al., 1999; Dinour, D., A. Knecht, I. Serban, and E.J. Holtzman. 2000. *J. Am. Soc. Neurol.* 11:3A; Igarashi, T., J. Inatomi, T. Sekine, Y. Yakeshima, N. Yoshikawa, and H. Endou. 2000. *J. Am. Soc. Nephrol.* 11:106A; Dinour et al., 2004). One patient has an inactivating homozygous missense mutation in which a Ser replaces Arg at position 298 in the cytoplasmic amino terminus of NBCe1-A (Igarashi et al., 1999). In expression studies using ECV304 cells, the authors found that this mutant NBC displayed only ~50% of wild-type transporter activity. This substitution is found at position 342 in the B and C variants. A second patient has a homozygous missense mutation in which a Leu replaces Ser at position 427 at the beginning of the first predicted transmembrane domain of NBCe1-A (Dinour et al., 2004). When expressed in oocytes, the mutant NBC displayed only ~10% of wild-type transporter activity. In a separate study, this mutant NBC was mistargeted to the apical instead of the basolateral membrane of polarized Madin-Darby canine kidney (MDCK) cells (Li et al., 2005).

According to the aforementioned studies, regions within the cytoplasmic amino and carboxy termini can influence the function, regulation, and expression of NBCe1 variants. However, a detailed comparison of the biophysical properties of all three variants with different amino and/or carboxy termini has yet to be performed. In the present manuscript, we used pH- and voltage-sensitive microelectrodes to characterize, for the first time, the function of rat brain NBCe1-B expressed in *Xenopus* oocytes. Subsequently, we used the two-electrode, voltage-clamp technique to compare the activities, as well as the ion and voltage dependencies of all three NBCe1 variants. Although all three variants have similar external ion and voltage dependencies, as well as plasma membrane expression levels as assessed by single oocyte chemiluminescence, the activity of the A variant is greater than the activities of the other two variants. According to structure–function analyses using whole-cell and macropatch recording techniques, the higher activity of A is due to its unique amino terminus. While the different amino termini influence function, one or more regions within the different carboxy termini contribute(s) to plasma membrane expression.

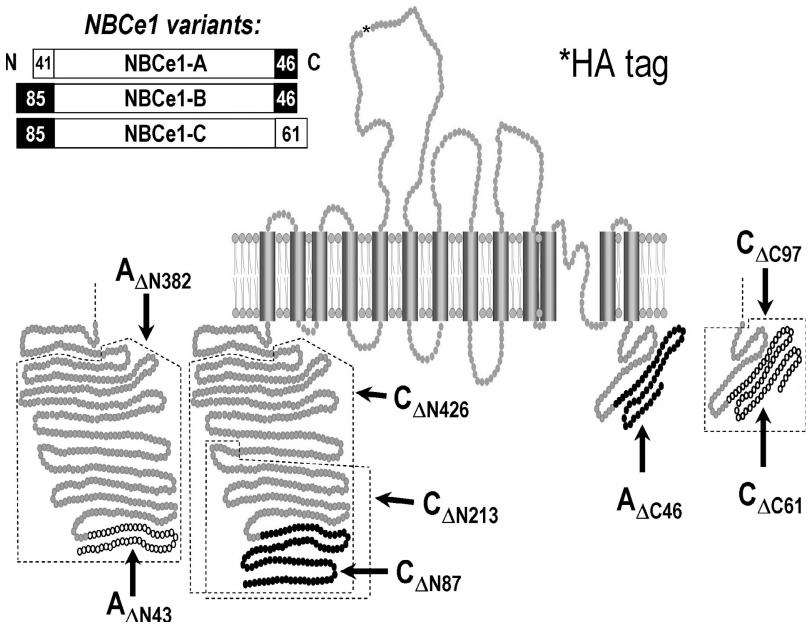

Figure 1. Wild-type and truncated rat NBCe1 variants. NBCe1-A, -B, and -C differ at the amino and/or carboxy termini. The putative membrane topology of NBCe1 is based on mapping of AE1 by Taylor et al. (2001). Truncations examined in this study include hemagglutinin (HA)-tagged NBCe1s with stretches of the cytoplasmic amino or carboxy terminus removed. (Inset, top left) At the amino terminus, NBCe1-A has 41 unique amino acids that differ from 85 amino acids in the B and C variants. At the carboxy terminus, NBCe1-C has 61 unique amino acids that differ from 46 amino acids in the A and B variants.

Portions of this work have been published in abstract form (Williams, J.B., and M.O. Bevensee. 2002. *FASEB J.* 16:A796; McAlear, S.D., J.B. Williams, and M.O. Bevensee. 2004. *FASEB J.* 18:A1022–A1023; Liu, X., S.D. McAlear, and M.O. Bevensee. 2005. *FASEB J.* 19:A142; McNicholas-Bevensee, C.M., X. Liu, S.D. McAlear, and M.O. Bevensee. 2006. *FASEB J.* 20:A1232).

MATERIALS AND METHODS

NBC Constructs and Mutagenesis

Wild-type NBCe1 Variants. We used cDNAs encoding NBCe1-A from rat kidney (Romero et al., 1998b), and NBCe1-C from rat brain (Bevensee et al., 2000) subcloned into the oocyte expression vector pTLNII as previously described. Full-length NBCe1-B, which was also previously identified from rat brain by RT-PCR (Bevensee et al., 2000), was constructed using convenient restriction enzymes to swap the unique carboxy terminus of full-length variant C in pTLNII with the carboxy terminus of variant B from a partial-length construct in pBluescript. For both wild-type and mutant constructs (see below), NBC expression was optimized by introducing a Kozak sequence (Kozak, 1986) at the initiator codon using PCR techniques and a Peltier thermal cycler (PTC-220 DNA Engine Dyad, MJ Research, Inc.). Sequence analysis and primer design were performed using either DNAsis (Hitachi Software) or Vector NTI Advance 9.0 (InforMax, Invitrogen), and all constructs were confirmed by bidirectional DNA sequencing (DNA Sequencing Core, Center for AIDS Research and the Genomics Core Facility, Heflin Center for Human Genetics, both at the University of Alabama at Birmingham).

HA-tagged NBCe1 Constructs. To insert the nine-residue hemagglutinin (HA) epitope (YPYDVPDYA) into NBCe1-C, we used the QuikChange PCR-based mutagenesis kit (Stratagene) to create a unique restriction site (Bsu36I) at base pair 1941 (residue 647) within the extracellular loop between transmembrane domains 5 and 6. A double-stranded pair of 5′- and 3′-phosphorylated primers encoding the HA epitope was flanked by Bsu36I sticky ends. Equal concentrations of the two primers were first denatured in a thermocycler (Genius FGEN05TP, Techne) by heating to 94°C (15 s), and then allowed to anneal by slowly cooling the reaction in increments of 2°C (15 s each) to 37°C. This double-stranded primer pair was then ligated into the engineered Bsu36I site in NBCe1-C. Because of the introduced Bsu36I cut sites, the inserted HA epitope in the protein was flanked by Asp and Gly. HA-tagged NBCe1-A and -B were constructed from the tagged NBCe1-C using convenient restriction enzymes.

Truncated NBCe1 Variants. Truncated NBCe1 constructs (see Fig. 1) were generated using PCR techniques and HA-tagged NBCe1 variants subcloned into pTLNII as templates. In generating amino-terminal truncations, we targeted residue 43 of the A variant and the homologous residue 87 of the C variant to optimize the Kozak sequence. NBCe1 constructs truncated at the carboxy terminus were generated by introducing a targeted stop codon using site-directed mutagenesis (QuikChange kit, Stratagene).

Functional Studies on NBCs

Generation of cRNA. pTLNII plasmids containing NBCe1 constructs were linearized with the restriction enzyme MluI. The linearized cDNA was then transcribed from the SP6 promoter using the SP6 transcription kit (Ambion), and the resulting cRNA was purified using the RNeasy kit (QIAGEN).

Isolation and Injection of Oocytes. Oocytes were harvested from female *Xenopus laevis* frogs using an approach very similar to that previously described (Romero et al., 1998b; Bevensee et al., 2000). A small incision was made in the abdominal cavity of the frog, and oocyte-containing segments of the ovarian lobe were removed. The segments were teased apart into small pieces and digested for 1.5–2 h in sterile Ca^{2+}-free ND96 containing 2 mg ml^{-1} collagenase A (Roche Applied Science). Subsequently, the dissociated oocytes were first washed in Ca^{2+}-free ND96, and then in Ca^{2+}-containing ND96 before healthy-looking stage V/VI oocytes were separated under a dissecting microscope (GZ6, Leica). The oocytes were incubated at 18°C in sterile ND96 containing 10 mM Na/pyruvate and 10 mg ml^{-1} gentamycin (Mediatech Inc.).

Oocytes were injected with 48 nl of either RNase-free H_2O or a cRNA solution using a "Nanoject II" microinjector (Drummond Scientific). Injected cells were incubated at 18°C in the aforementioned

oocyte media, and experiments were performed at room temperature at least 2 d after injection.

pH_i and V_m Experiments. Injected oocytes were placed in a flowthrough chamber connected to a custom-designed, dual-bank, solution delivery system. Main solution lines from two banks, which are each connected to six solution lines via a six-way rotary manifold, were directed to a two-position, Eagle four-way miniature solenoid valve with five ports (Clippard Instrument Laboratory). During experiments, solution from one bank was directed to the chamber, and solution from the other bank was directed to waste for priming purposes. Changing solutions delivered to the chamber occurred by pneumatically alternating between the two valve positions.

For simultaneous pH_i and voltage recordings, microelectrodes were pulled from borosilicate glass capillaries (G200F-4, Warner Instruments) with a Brown-Flaming micropipette puller (P-80 or P-97, Sutter Instruments). For pH electrodes, pulled acid-washed capillaries were subsequently baked at 200°C and silanized with *bis*-(methylamino)dimethylsilane (Fluka). Electrode tips were filled with hydrogen ionophore I-cocktail B (Fluka), and then the electrodes were backfilled with a pH 7.0 solution containing (in mM): 150 NaCl, 40 KH_2PO_4, and 23 NaOH. pH electrodes were then connected to one channel of a high-impedance electrometer (FD223, WPI). Voltage electrodes were filled with a saturated KCl solution and connected to a second channel. The microelectrodes typically had resistances of 1–3 MΩ. The pH signal was obtained with a four-channel electrometer (Biomedical Instrumentation Laboratory, Department of Cellular and Molecular Physiology, Yale University, New Haven, CT) that subtracts the potential of the voltage electrode from the potential of the pH electrode. A miniature calomel electrode (Accumet, Fisher Scientific) filled with saturated KCl served as the reference for the voltage electrode. Data were acquired and plotted using custom-designed software written by Mr. Duncan Wong for the Boron laboratory (Department of Cellular and Molecular Physiology, Yale University).

Two-electrode, Voltage-clamp Experiments. Voltage-sensitive and current-passing microelectrodes were pulled from borosilicate glass capillaries (G200F-4 or G83165T-4, Warner Instruments) with a micropipette puller (P-80 or P-97, Sutter Instruments or PC-10, Narishige, Tokyo, Japan). The electrodes were filled with saturated KCl and attached to the OC-725C voltage-clamp apparatus (Warner Instruments). Electrode resistances were typically 1-3 MΩ for the voltage electrodes, and 0.1–0.6 MΩ for the current electrodes. For experiments at a fixed holding potential of −60 mV, data were obtained at a filtering frequency of either 8–10 or 800 Hz with an 8-pole Bessel filter (LFP-8, Warner Instruments) and a sampling frequency of 30 Hz or 2 kHz, respectively. For the current-voltage (I-V) relationships shown, the data were obtained at a filtering frequency of 800 Hz and a sampling frequency of 2 kHz. The voltage-step protocol for the I-V plots shown included 12 sweeps in which the voltage was held at −60 mV for 60 ms, then stepped to one of 12 voltages (–200 mV to 20 mV in increments of 20 mV) for 20 ms, and finally returned to −60 mV for 20 ms before the next sweep. After obtaining each I-V plot, we confirmed that the oocyte was electrically tight by turning off the voltage clamp and verifying that the spontaneous V_m was close to the acquired reversal potential (Virkki et al., 2002). Data acquired with the ClampEx software (Axon Instruments pClamp 8.2, Molecular Devices, San Jose, CA) were digitized with a 1322A interface (Axon Instruments), and then analyzed with ClampFit software (pClamp 8.2, Axon Instruments).

Inside-out macropatch experiments. Macropatch studies were performed on oocytes using a modification of the technique described by Hilgemann (1995). Patch pipettes were pulled from N-51-A borosilicate glass capillaries (O.D. 0.084 in. or 0.064 in., Drummond) using a PC-10 micropipette puller (Narishige). Tips gently broken to 10–12 μm were plunged into a bead of melted 8161 Corning glass (G86165T-4, Warner Instruments) fixed to 30-gauge, MF-9 platinum wire (Technical Products International Inc.), which was transiently heated by passing current. A break at the tip resulted from the wire retracting as it cooled. The process of heating the glass bead, plunging the tip, and cooling the wire was repeated until a satisfactory jagged-free tip of ∼14 μm in diameter was obtained. Pipette resistances were ∼4 MΩ.

Experiments were performed at room temperature (∼23°C) in a flowthrough chamber on the stage of an inverted microscope (DMIRB, Leica). All solutions contained low Cl^- (2 mM) to minimize contaminating endogenous Cl^- currents in the oocyte (Machaca et al., 2002; Weber, 2002). Immediately before experiments, pipettes were backfilled with solution containing 5% CO_2/33 mM HCO_3^-. Access to the plasma membrane was obtained by shrinking the oocyte in a hypertonic solution (see below) and then removing the vitelline membrane with fine forceps. GΩ seals were obtained at a negative holding potential (V_p = −50 mV), and solution flow was initiated after patch excision. NBC currents were similar from patches obtained from either the animal or vegetal pole of the oocyte.

Currents were obtained using an Axopatch 200B patch-clamp amplifier (Axon Instruments). Low-pass (1 kHz, internal filter) currents were digitized with a Digidata-1322A interface (Axon Instruments) at a sampling frequency of 5 kHz. Clampex software (pClamp 8.2, Axon Instruments) was used for data acquisition and analysis. Seal stability was routinely monitored throughout the experiment by measuring both membrane capacitance (using the membrane test function of Clampex) and seal resistance. For the figures shown, current recordings were further filtered at 100 Hz (8-pole Bessel filter), and subjected to data reduction (substitute average by a factor of four) using Clampfit (pClamp 8.2, Axon Instruments). Data were exported to Microsoft Excel 2002 for analysis and Origin 7.5 (OriginLab Corporation) for graphing.

Solutions

Two-electrode, Voltage-clamp Experiments. The standard ND96 solution (pH 7.5) contained (in mM): 96 NaCl, 2 KCl, 1 $MgCl_2$, 1.8 $CaCl_2$, 5 HEPES, 2.5 NaOH. In the standard 5% CO_2/33 mM HCO_3^- solution, 33 mM NaCl was replaced with an equimolar amount of $NaHCO_3$, and the solution was equilibrated with 5% CO_2/95% O_2 to pH 7.5. In the low Cl^- (7.6 mM)-containing ND96 and 5% CO_2/33 mM HCO_3^- solutions used in the bicarbonate and voltage dependence experiments, the NaCl was replaced with equimolar amounts of sodium gluconate. 7.6 mM Cl^- was kept constant in solutions containing different amounts of HCO_3^- by replacing sodium gluconate with equimolar amounts of $NaHCO_3$. pH of the different HCO_3^--containing solutions was maintained at 7.5 by equilibrating the solutions with appropriate mixtures of CO_2/O_2. In the Na^+ dependence experiments, equimolar Na^+ was replaced with $NMDG^+$.

Inside-out Macropatch Experiments. The hyperosmotic solution used to remove the vitelline membrane contained (in mM): 220 $NMDG^+$, 220 aspartic acid, 2 $MgCl_2$, 10 EGTA, and 10 HEPES. The solution was titrated to pH 7.2 with $NMDG^+$.

For inside-out macropatch experiments, the 2 mM-Cl^-, ND96 solution contained (in mM) 96 sodium cyclamate, 2 mM KOH, 2 mM cyclamic acid, 1 mM $MgCl_2$, 1.8 mM calcium cyclamate, 5 mM HEPES, and was adjusted to pH 7.5 with NaOH. In the 2-mM Cl^- solution containing 5% CO_2/33 mM HCO_3^-, 33 mM sodium cyclamate was replaced with an equimolar amount of $NaHCO_3$, and the solution was equilibrated with 5% CO_2/95% O_2

to pH 7.5. For all experiments, the 2 mM Cl^- solution containing 5% CO_2/33 mM HCO_3^- served as the patch pipette solution.

All chemicals were obtained from Sigma-Aldrich unless otherwise specified. According to packaging information, 4,4′-diisothiocyanatostilbene-2,2′ disulfonate (DIDS) was at least 80% pure, a value factored into making DIDS-containing solutions.

Expression Studies on NBCs

Immunoblotting. Similar to previously described (Schmitt et al., 1999; Bevensee et al., 2000), each oocyte was homogenized in a buffer containing protease inhibitors, and the suspension was centrifuged to remove cell debris and nuclei. Proteins were separated by SDS-7.5% PAGE (Ready Gels Precast Gels, Bio-Rad Laboratories) and transferred to an Immobilin-P PVDF membrane (Millipore). The membrane was probed for 1–2 h with a 1:200 dilution of a rabbit polyclonal antibody (Rab3A) to the amino terminus of NBCe1 (Schmitt et al., 1999), and then for 1 h with a 1:10K dilution of the secondary antibody, goat αrabbit-IgG coupled to horseradish peroxidase (HRP) (Jackson ImmunoResearch Laboratories). Bound HRP was detected by chemiluminescence (SuperSignal, Pierce Chemical Co.) before being exposed to HXR Film (Hawkins X-Ray Supply).

Single-oocyte Chemiluminescence. To evaluate the expression of NBCs at the oocyte plasma membrane, we used the single-oocyte chemiluminescence (SOC) technique pioneered by the Jan lab (Zerangue et al., 1999; Margeta-Mitrovic et al., 2000) and used by others (Yoo et al., 2003) to quantitate a hemagglutinin (HA)–tagged protein expressed at the cell surface. This technique employs enzyme amplification with a chemiluminescence substrate and sensitive, linear detection with a luminometer. As reported by Yoo et al. (2003), there is a linear relationship between surface expression detected by SOC and functional activity of the K^+ channel, ROMK (Kir 1.1).

The following protocol with sterile ND96 solutions was performed on injected oocytes incubated at 4°C. Oocytes were fixed with 4% paraformaldehyde in ND96 for 15 min, rinsed 3×5 min with equal volumes of ND96, and then incubated for 30 min (or overnight) in a 1% BSA-ND96 blocking solution (used in subsequent antibody incubation steps). Fixing the oocytes with paraformaldehyde does not appreciably increase their permeability to the HA antibody. As shown in Results, there was no detectable labeling of truncated, HA-tagged NBCe1 proteins that fail to traffic to the plasma membrane, but were clearly present in a microsomal fraction based on immunoblot analyses. Fixed oocytes were incubated for 1 h in a 1:100 dilution of the rat monoclonal α-hemagglutinin antibody (Roche), and then for 1 h in a 1:400 dilution of the secondary antibody, goat α-rat IgG-HRP (Jackson ImmunoResearch Laboratories). For chemiluminescence readings, each oocyte was transferred to an eppendorf tube, and the transferred solution was replaced with 50 μl SuperSignal Elisa Femto substrate (Pierce Chemical Co.). The eppendorf tube was placed in a luminometer (TD-20/20, Turner Designs) and luminescence was measured 15 s later.

Statistics

Means between groups of data were compared using one-factor analysis of variance (ANOVA), as well as paired or unpaired forms of the Student's *t* test (Microsoft Excel 2002). $P < 0.05$ is considered significant. Rates of pH_i recoveries were determined by linear fits to pH_i vs. time data using a least-squares method. With Origin 7.5 software (OriginLab), Na^+ dependence data were fit using Michaelis-Menten enzyme kinetics, and HCO_3^--dependence data were fit using a modified form of the Michaelis-Menten equation that includes a linear component (Grichtchenko et al., 2000). Comparisons of fits were performed using Origin 7.5 software (OriginLab).

RESULTS

Functional Expression of Rat Brain NBCe1-B in Oocytes

At the time the cDNA encoding rat brain NBCe1-C was cloned by homology and the protein characterized as an electrogenic NBC when expressed in oocytes, rat brain NBCe1-B was also identified (Bevensee et al., 2000). The amino acid sequence of rat brain NBCe1-B is 96% identical to that of human heart NBCe1-B, which has been characterized as a stilbene-sensitive, electrogenic NBC when expressed in oocytes (Choi et al., 1999). In the present manuscript, we expressed the rat brain version of NBCe1-B in oocytes and evaluated NBC function using pH- and voltage-sensitive microelectrodes.

At the onset of the experiment shown in Fig. 2 A, an oocyte injected with rat brain NBCe1-B and bathed in a nominally CO_2/HCO_3^--free, HEPES-buffered solution (ND96, pH 7.5) had a resting pH_i of ~7.32 (top trace) and a V_m of −55 mV (bottom trace). Exposing the oocyte to a solution containing 1.5% CO_2/10 mM HCO_3^- (pH 7.5) elicited an initial decrease in pH_i (ab) due to CO_2 entry and subsequent formation of H^+ in the cell. The pH_i then increased (bc) due to NBC-mediated HCO_3^- transport into the oocyte. The mean pH_i recovery rate at a pH_i of 7.12 ± 0.02 (after the initial CO_2-induced acidification) was $7.1 \pm 0.8 \times 10^{-5}$ pH units s^{-1} ($n = 6$). This pH_i recovery was blocked (cd) by 200 μM DIDS, an inhibitor of bicarbonate transporters. As shown in Table I, stilbenes reduced the rate of pH_i recovery under different CO_2/HCO_3^- conditions by a mean of 76 ± 7.5% (range: 58–100%). Inhibition of the pH_i recovery was at least partially reversible (de) when DIDS was removed. Returning the oocyte to ND96 caused pH_i to increase rapidly (ef) due to the net conversion of intracellular H^+ and HCO_3^- to H_2O and CO_2, which exited the cell. The final resting pH_i was higher than the initial value, an observation consistent with net NBC-mediated HCO_3^- influx during segment be.

The voltage changes in the NBC-expressing oocyte exposed to CO_2/HCO_3^- and then DIDS (Fig. 2 A, bottom trace) demonstrate that NBCe1-B is electrogenic. Applying the CO_2/HCO_3^- solution elicited an ~17-mV hyperpolarization (a′b′) that is consistent with NBC transporting more bicarbonate than sodium into the oocyte. In the same six experiments summarized above, the mean hyperpolarization elicited by 1.5% CO_2/10 mM HCO_3^- was 25 ± 8 mV. Also consistent with electrogenic Na/HCO_3^- cotransport activity was the ~10-mV depolarization seen when the oocyte in CO_2/HCO_3^- was exposed to 200 μM DIDS (c′).

The experimental maneuvers shown in Fig. 2 A had markedly different effects on pH_i and V_m of the H_2O-injected control oocyte shown in Fig. 2 B. As shown in the top trace, the 1.5% CO_2/10 mM HCO_3^- solution elicited the initial pH_i decrease (ab), but no subsequent pH_i recovery (bc). At a mean pH_i of 7.08 ± 0.07, the

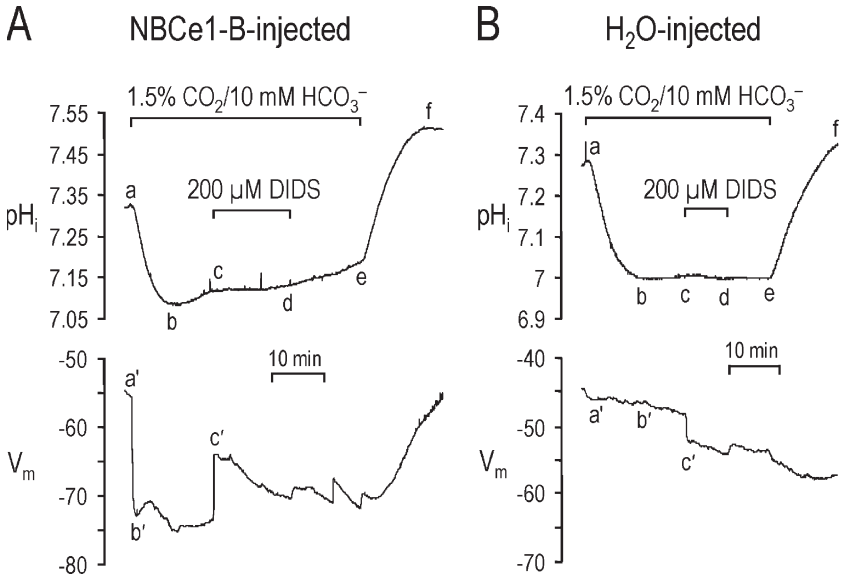

Figure 2. Activity of rat brain NBCe1-B expressed in an oocyte. (A) pH_i (top trace) and voltage (bottom trace) were measured simultaneously in an NBCe1-B–injected oocyte that was initially bathed in a nominally HCO_3^--free, HEPES-buffered solution. The oocyte was exposed to a solution containing 1.5% CO_2/10 mM HCO_3^- during segment ae. Electrogenic NBC activity was evident from the instantaneous hyperpolarization (b'), and the pH_i recovery (bc) following the initial CO_2-induced acidification (ab). DIDS blocked the pH_i recovery (cd), and partially reversed the hyperpolarization (c'). (B) The same experimental protocol in panel A was performed on an H_2O-injected oocyte. Exposing the oocyte to CO_2/HCO_3^- had no effect on V_m (a'b'), and elicited no pH_i recovery (bc) following the initial decrease in pH_i (ab). 200 μM DIDS generated only a small hyperpolarization (c').

mean pH_i recovery rate of $2.1 \pm 1.2 \times 10^{-5}$ pH units s^{-1} ($n = 4$) was 3.4-fold less ($P < 0.01$) than the rate seen in NBCe1-B-expressing oocytes. Furthermore, 200 μM DIDS in the presence of CO_2/HCO_3^- had little effect on the low, sustained pH_i (cd). Returning the oocyte to ND96 caused pH_i to increase and return to approximately the initial resting value (ef). The voltage changes in the control oocyte were equally unimpressive (bottom trace). CO_2/HCO_3^- had no effect on V_m (a′b′), and DIDS only caused a small hyperpolarization (c′), consistent with inhibition of an endogenous Cl^- conductance. In the same four experiments summarized above, the mean HCO_3^--induced hyperpolarization of 1.5 ± 0.3 mV was 17-fold less than the hyperpolarization seen in NBCe1-B–expressing oocytes.

To increase the activity of NBCe1-B, we performed additional pH_i/V_m experiments using solutions containing 33 mM HCO_3^- and equilibrated with 5% CO_2 to maintain pH at 7.5. The mean pH_i-recovery rate at a pH_i of 6.87 ± 0.03 was $12.0 \pm 2.5 \times 10^{-5}$ pH units s^{-1} ($n = 11$). At a similar pH_i (6.84 ± 0.03) in H_2O-injected oocytes, the mean pH_i recovery rate of $4.3 \pm 1.9 \times 10^{-5}$ pH units s^{-1} ($n = 6$) was 2.8-fold less ($P = 0.01$). In these same experiments, the mean hyperpolarization elicited by 5% CO_2/33 mM HCO_3^- was 53 ± 4.8 mV in NBC-expressing oocytes, and only 0.5 ± 0.5 mV in H_2O-injected oocytes. In summary, rat brain NBCe1-B expressed in oocytes is electrogenic, stilbene-sensitive, and activated by CO_2/HCO_3^-. As described below in voltage-clamp experiments, the transporter is also Na^+ dependent. All these characteristics are hallmarks of an electrogenic Na/HCO_3 cotransporter (see Romero et al., 2004).

Voltage Dependencies of the NBCe1 Variants

To study the electrogenicity of the NBCe1 variants in more detail, we used the two-electrode, voltage-clamp technique to examine current–voltage (I-V) relationships of all three NBCe1 variants. In each experiment, I-V relationships were obtained from oocytes first bathed in a low Cl^-, ND96 solution, and then after 10 min in 5% CO_2/33 mM HCO_3^- (to allow for intracellular equilibration of the physiological buffer). In some experiments, I-V plots were subsequently obtained after 2 min in the CO_2/HCO_3^- solution containing 200 μM DIDS. The HCO_3^--dependent I-V plot for an NBC is the

TABLE I

Stilbene Sensitivity of the pH_i Recovery Rate when Oocytes Expressing NBCe1-B Are Exposed to CO_2/HCO_3^-

Experiment	CO_2 /HCO_3^-	Stilbene	pH_i[a]	dpH_i/dt ($\times 10^{-5}$) before stilbene	dpH_i/dt ($\times 10^{-5}$) with stilbene	% inhibition
1010725D	1.5%/10 mM	0.2 mM DIDS	6.99	22.2	7.1	68
1010725E	1.5%/10 mM	0.2 mM DIDS	7.12	10.3	0.0	100
1010621C	1.5%/10 mM	0.5 mM DIDS	7.33	3.8	1.6	58
1010627D	1.5%/10 mM	1.0 mM DNDS	7.11	7.9	0.2	97
1010628B	5.0%/33 mM	1.0 mM DNDS	7.0	14.0	5.2	63
1010628C	5.0%/33 mM	1.0 mM DNDS	7.05	15.6	5.4	65

DNDS, 4,4′-dinitrostilbene-2,2′ disulfonate.

[a]Intracellular pH at the time of stilbene inhibition.

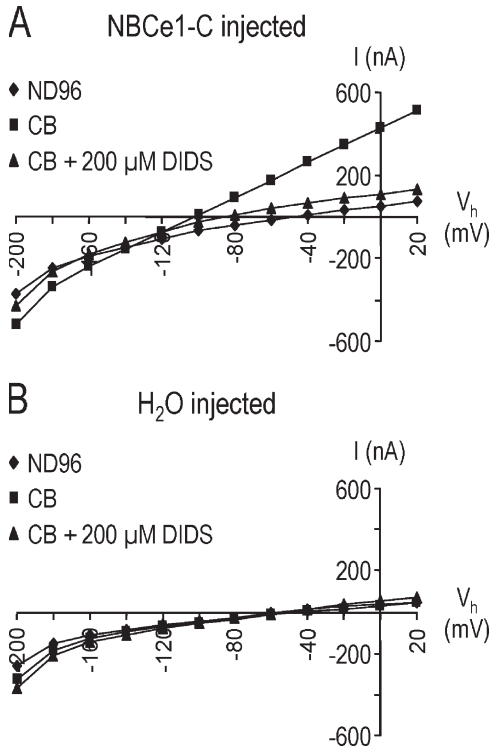

Figure 3. Current–voltage (I-V) relationship of NBCe1-C expressed in oocytes. (A) I-V plots were obtained from an NBCe1-C–expressing oocyte initially bathed in ND96 (diamonds), followed by 10 min in 5% CO_2/33 mM HCO_3^- (CB) (squares), and then after 2 min in the CO_2/HCO_3^- solution containing 200 μM DIDS (triangles). (B) The same experimental protocol in A was performed on an H_2O-injected oocyte.

difference between the I-V plots obtained in the presence and absence of CO_2/HCO_3^-, after subtracting the corresponding HCO_3^--dependent I-V plot obtained from batch-matched H_2O-injected eggs.

An experiment performed on an oocyte expressing NBCe1-C is shown in Fig. 3 A. NBC currents obtained at potentials from −200 to +20 mV were larger in the presence of 5% CO_2/33 mM HCO_3^- (squares) than in ND96 (diamonds). The larger currents were particularly evident at voltages more positive than −80 mV. In the presence of DIDS, the I-V plot (triangles) reverted back to that seen with ND96. DIDS-sensitive HCO_3^- currents were not observed in an H_2O-injected control oocyte (Fig. 3 B). I-V plots looked similar for the control oocyte exposed to ND96 and $CO_2/HCO_3^- \pm$ DIDS.

In Fig. 4 A, the average I-V relationships are shown for NBCe1-A (closed diamonds), -B (open squares), and -C (closed triangles). There are four noteworthy observations. First, the currents for the A variant are the largest. Second, all three I-V plots display a slight outward rectification. Third, the I-V plots for the B and C variants are nearly identical. The final observation is that the E_{rev} is ∼−85 mV for A (Fig. 4 A), but markedly more negative for B (∼−155 mV) and C (∼−170 mV) (Fig. 4 A, boxed inset). Although the more negative E_{rev} values are consistent with different Na:HCO_3^- transport stoichiometries, a more likely explanation is different transmembrane Na^+ and HCO_3^- gradients established by the NBCs. For example, compared to A, the less active B and C variants generate a smaller increase in $[Na^+]$ and $[HCO_3^-]$ on the cytosolic side of the membrane, and therefore a more negative V_m for B and C is required to drive transport in the reverse direction out of the cell. We tested this possible explanation by injecting a smaller amount of NBCe1-A cRNA to reduce the magnitude of the whole-cell A current. Indeed, oocytes exhibiting smaller A currents displayed a negative shift in E_{rev} (Fig. 4 B, open diamonds). For comparison, the I-V relationship for NBCe1-A shown in A is replotted in Fig. 4 B (closed diamonds).

To minimize the influence of different transmembrane gradients, we compared the voltage dependencies of the three variants under similar transporter-mediated whole-cell currents. NBCe1-B and -C currents were increased by injecting oocytes with NBC cRNAs containing a modified Kozak sequence, whereas NBCe1-A currents were decreased by injecting oocytes with less cRNA. As shown in Fig. 4 C, the voltage dependencies of the three variants exhibiting comparable NBC-mediated currents are very similar.

Expression of the NBCe1 Variants at the Plasma Membrane of the Oocyte

Activity of Hemagglutinin-tagged NBCe1 Variants. The higher activity of NBCe1-A compared to the B and C variants shown in Fig. 4 A could be due to differences in plasma membrane expression. We therefore used the SOC technique with HA-tagged NBCe1 constructs to assess surface expression. We first tested the function of the tagged constructs expressed in oocytes. As shown in Fig. 4 B, there is no difference between the voltage dependencies of the untagged NBCe1-A (closed diamonds) redrawn from Fig. 4 A, and the HA-tagged transporter (NBCe1-A_{HA}, closed squares). We performed additional studies to compare the function of tagged NBCe1-C. In pH_i/V_m and voltage-clamp studies in which oocytes expressing either tagged or untagged NBCe1-C were exposed to 5% CO_2/33 mM HCO_3^-, both groups displayed similar NBC-mediated hyperpolarizations, pH_i recovery rates following the initial CO_2-induced acidification, HCO_3^--induced outward currents under voltage-clamp conditions, and I-V relationships. In conclusion, the introduced HA epitope does not alter NBCe1 activity.

Comparing Function and Surface Expression of NBCe1 Variants. We expressed HA-tagged NBCe1-A and NBCe1-C in oocytes, and then evaluated both transporter function with the two-electrode, voltage-clamp technique, and expression with the SOC technique. In our functional

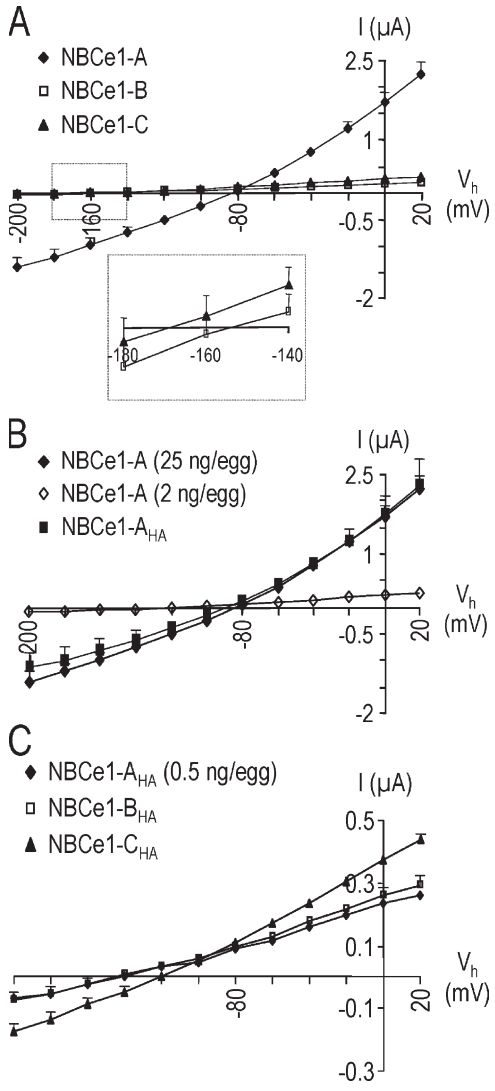

Figure 4. I-V relationships of the three NBCe1 variants. (A) HCO_3^--dependent I-V plots were obtained from oocytes expressing NBCe1-A (closed diamonds), NBCe1-B (open squares), and NBCe1-C (closed triangles). For each data point, $n \geq 11$. (Inset) The I-V plots are magnified near the reversal potentials ($I_M = 0$) for NBCe1-B and C. (B) HCO_3^--dependent I-V plots from oocytes injected with 25 ng of NBCe1-A cRNA (closed diamonds, redrawn from A), 2 ng of NBCe1-A cRNA (open diamonds, $n = 3$), or 25 ng of HA-tagged NBCe1-A_{HA} cRNA (closed squares, $n = 6$). (C) HCO_3^--dependent I-V plots from oocytes injected with 0.5 ng of NBCe1-A_{HA} cRNA (closed diamonds, $n = 3$), 25 ng of NBCe1-B_{HA} cRNA (open squares, $n = 4$), or 25 ng of NBCe1-C_{HA} cRNA (closed triangles, $n = 4$). Error bars smaller than symbols are not shown.

assay, we monitored NBC-mediated outward currents in oocytes voltage clamped at −60 mV and exposed to 5% CO_2/33 mM HCO_3^-. In contrast to an oocyte injected with H_2O, an oocyte injected with either the A or C variant displayed an outward current when exposed to 5% CO_2/33 mM HCO_3^- (Fig. 5 A). The A and C currents differed in the following three ways. First, the A-mediated current was ~4.5-fold larger than the C-mediated current. Second, the A-mediated current peaked faster than the C-mediated current. Finally, in contrast to the C-mediated current, the A-mediated current decayed after its peak. The current decay is consistent with reduced transport in response to the buildup of substrate or a pH_i increase at the inner surface of the oocyte membrane (and opposite changes at the outer surface of the membrane). According to subsequent data presented, the more active the transporter (as judged by the magnitude of the peak HCO_3^--induced current), the faster the decay. As summarized in Fig. 5 B on two batches of day-matched oocytes, the mean H_2O-subtracted, peak CO_2/HCO_3^--induced current was 4.3-fold larger in oocytes expressing NBCe1-A (874 ± 82 nA, $n = 8$) compared to NBCe1-C (201 ± 4 nA, $n = 7$). The larger NBC-mediated current seen with NBCe1-A compared to C is consistent with the I-V plot data shown in Fig. 4 A.

We used the same two batches of oocytes to examine plasma membrane NBC expression with the SOC technique. For each batch, the luminescence for each oocyte was normalized to the mean luminescence of oocytes expressing NBCe1-A. As expected, the mean normalized luminescence (Norm. Lum.) for A- or C-expressing oocytes was considerably higher than the mean value for H_2O-injected oocytes (Fig. 5 C). These readings are specific for the anti-HA antibody because in a separate experiment (not depicted), luminescence was not observed when the anti-HA antibody was preabsorbed with an equal amount (1 mg ml^{-1}) of the HA peptide. As shown by the second and third bars in Fig. 5 C, the mean Norm. Lum. was the same for the two NBCe1 variants ($P > 0.3$).

Similar functional and expression studies were performed on the HA-tagged NBCe1-B variant. The mean CO_2/HCO_3^--induced current was threefold smaller in oocytes expressing NBCe1-B (258 ± 10 nA, $n = 6$) compared to NBCe1-A (787 ± 57 nA, $n = 7$). According to SOC analysis, the mean Norm. Lum. was identical for oocytes expressing the B variant (1.01 ± 0.07, $n = 5$) and A variant (1.00 ± 0.09, $n = 5$). Therefore, the lower activity of B or C vs. A cannot be explained by lower plasma membrane expression.

External Ion Dependencies of the NBCe1 Variants

The increased activity of NBCe1-A compared to the B and C variants may be due to a higher affinity for HCO_3^- and/or Na^+. In the following two sections, we compare –for each NBCe1 variant– the external HCO_3^- and Na^+ dependencies.

External HCO_3^- Dependencies. We used an approach introduced by Grichtchenko et al. (2000) to determine the HCO_3^- dependencies of NBCe1s expressed in oocytes voltage clamped at −60 mV. NBC-mediated outward currents were recorded when oocytes were exposed to either 5% CO_2/33 mM HCO_3^- (standard HCO_3^-),

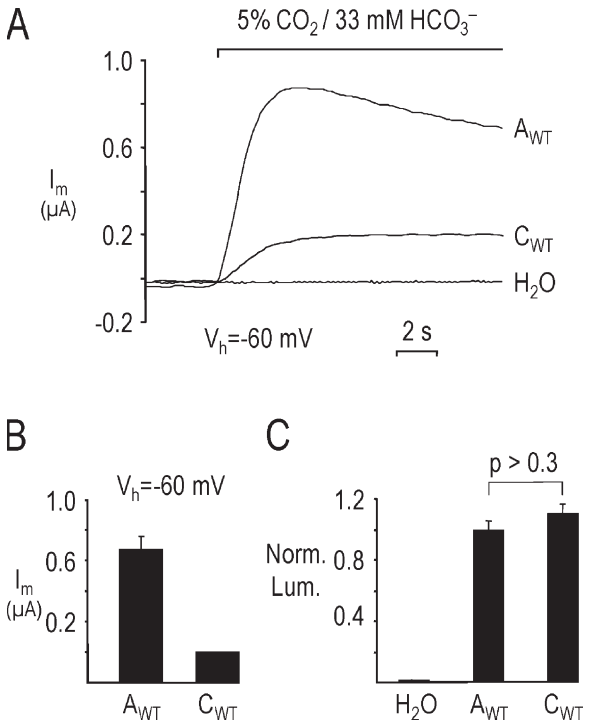

Figure 5. Larger HCO_3^--induced currents in oocytes expressing NBCe1-A than NBCe1-C. (A) A 5% CO_2/33 mM HCO_3^- solution elicited an outward current in the NBCe1-A–expressing oocyte (A_{WT}) that was 4.5-fold higher than the current in the NBCe1-C-expressing oocyte (C_{WT}). An H_2O-injected oocyte displayed no HCO_3^--induced outward current. (B) Summary of H_2O-subtracted, HCO_3^--induced currents from experiments similar to those shown in A. $n \geq 7$ from two batches of oocytes. (C) The mean normalized luminescence (Norm. Lum.) was similar for the A and C variants. $n \geq 12$ from two batches of oocytes.

or solutions containing different HCO_3^- concentrations and equilibrated with appropriate CO_2/O_2 mixtures to maintain a pH of 7.5. All solutions contained 7.6 mM Cl^- as described above.

Results from an oocyte expressing NBCe1-C are shown in Fig. 6 A. The oocyte was initially bathed in the normal Cl^- (103.6 mM), HEPES-buffered solution and voltage clamped at −60 mV. Exposing the oocyte to a solution containing 7.6 mM Cl^- generated a slow outward current (ab), possibly due to a small gluconate conductance. Exposing the oocyte to solutions containing different [HCO_3^-]s elicited rapid NBC-mediated outward currents (c-i). Currents were larger at progressively higher [HCO_3^-]s (h vs. d vs. e vs. f). Each non-33 mM HCO_3^- exposure was flanked by standard HCO_3^- exposures. A similar experiment performed on an H_2O-injected oocyte is shown in Fig. 6 B. The CO_2/HCO_3^- solutions elicited only slow inward currents (c-i).

Using data from experiments similar to those shown in Fig. 6 A, we plotted the HCO_3^- dependencies of NBCe1-B and -C. To correct for current drifts during experiments, as well as any differences in NBC expression among oocytes, we normalized the current elicited by each HCO_3^- exposure to the mean current elicited by the flanking standard HCO_3^- exposures. Corresponding currents obtained from H_2O-injected oocytes were subtracted before normalization. The external HCO_3^- dependencies are shown for NBCe1-B (Fig. 6 C) and NBCe1-C (Fig. 6 D). The data for both variants are well fit using a model that combines a Michaelis-Menten mechanism with a linear component, as has been reported for rat kidney NBCe1-A (Grichtchenko et al., 2000). The external HCO_3^- dependencies of the B and C variants are nearly identical. For NBCe1-B, the apparent K_M for HCO_3^- is 4.68 ± 0.47 mM and the normalized V_{max} is 0.92 ± 0.03 (n = 24 from six oocytes). For NBCe1-C, the apparent K_M for HCO_3^- is 4.31 ± 0.46 mM and the normalized V_{max} is 0.88 ± 0.03 (n = 24 from six oocytes). These values for the B and C variants are very similar to our values of apparent K_M (6.90 ± 3.04 mM) and normalized V_{max} (0.96 ± 0.12) (n = 10 from three oocytes) obtained for the A variant. Furthermore, our values for NBCe1-A are nearly identical to the values of apparent K_M (6.5 mM) and normalized V_{max} (0.97) previously reported for NBCe1-A (Grichtchenko et al., 2000).

We also examined the bicarbonate dependence of an NBCe1-A/C chimera that contains the 41 amino-terminal residues of the A variant and the 61 carboxy-terminal residues of the C variant. In these studies, the A/C chimera exhibited a mean outward current (1240 ± 103 nA, n = 5) similar to that of wild-type NBCe1-A (1096 ± 296 nA, n = 3) when the oocytes were exposed to 5% CO_2/33 mM HCO_3^-. This chimera also had a similar apparent K_M for HCO_3^- of 5.33 ± 0.54 mM and normalized V_{max} of 1.00 ± 0.04 (n = 17 from five oocytes). In conclusion, the external HCO_3^- dependencies are no different ($P \geq 0.89$) for all three NBCe1 variants and the NBCe1-A/C chimera. Therefore, the larger NBC-mediated current seen with NBCe1-A compared to the B and C variants is not due to a higher HCO_3^- affinity.

External Na^+ Dependencies. We used a similar approach to the one described above to determine the external Na^+ dependencies of the NBCe1 variants. In our assay, we examined the magnitudes of the NBC-mediated outward currents elicited by 5% CO_2/33 mM HCO_3^- solutions containing various [Na^+]s. Our experimental protocol minimized changes in intracellular [Na^+] ([Na^+]$_i$) by minimizing the time oocytes spent in reduced [Na^+]s.

Results from an oocyte expressing NBCe1-C are shown in Fig. 7 A. The voltage-clamped oocyte was initially bathed in ND96 and then exposed to 5% CO_2/33 mM HCO_3^- solutions containing different amounts of Na^+. These HCO_3^- exposures elicited rapid NBC-mediated outward currents (a-i), which were smaller at progressively lower concentrations of Na^+ (b vs. d vs. f vs. h).

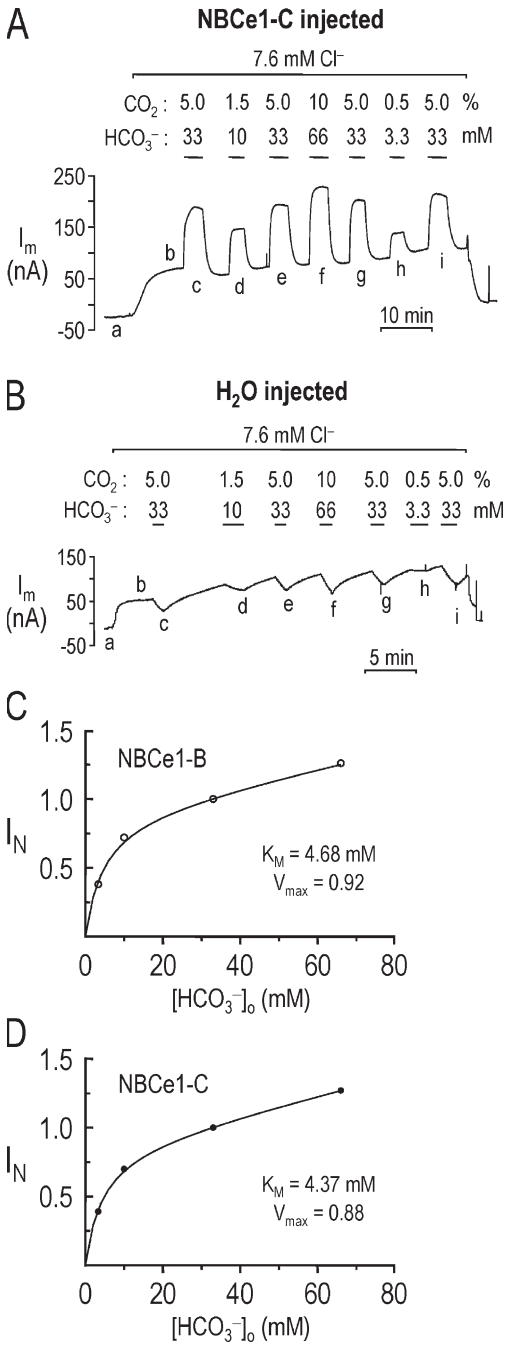

Figure 6. External HCO_3^--dependencies of NBCe1-B and -C. (A) A voltage-clamped oocyte ($V_h = -60$ mV) expressing NBCe1-C was exposed to different HCO_3^--containing solutions at a constant [Cl^-] of 7.6 mM. (B) The experimental protocol used in A was performed on an H_2O-injected oocyte. (C) Normalized HCO_3^--induced currents as a function of external [HCO_3^-] for oocytes expressing NBCe1-B ($r^2 = 0.99$). HCO_3^--induced outward currents in experiments similar to that in A were normalized to the mean currents elicited by the flanking exposures to the standard 5% CO_2/33 mM HCO_3^- solution. (D) Normalized HCO_3^--induced currents as a function of external [HCO_3^-] for oocytes expressing NBCe1-C ($r^2 = 0.99$).

Using an approach similar to that described above for our bicarbonate-dependence experiments, each low-Na^+, HCO_3^- exposure was flanked by full-Na^+ (98.5 mM) HCO_3^- exposures. A similar experiment on an H_2O-injected oocyte subjected to the same experimental protocol is shown in Fig. 7 B. The CO_2/HCO_3^- solutions of different Na^+ concentrations elicited only small outward currents.

One noteworthy observation (unpublished data) with oocytes expressing NBCe1-A was the presence of a Na^+-independent, outward current elicited by CO_2/HCO_3^- that was not seen in H_2O-injected oocytes. In the absence of external Na^+, the 33 mM HCO_3^- solution elicited a mean outward current in A-expressing oocytes (153 ± 48 nA, $n = 4$) that was 13-fold larger ($P = 0.03$) than that seen in H_2O-injected oocytes (12 ± 3 nA, $n = 4$), and 18 ± 5% of the total HCO_3^- current in "full" 98.5 mM Na^+. This Na^+-independent HCO_3^- current, which was not seen in oocytes expressing NBCe1-B (12 ± 3 nA, $n = 6$) or NBCe1-C (19 ± 3 nA, $n = 10$), may be due to transporter slippage as described for H^+ pumps, neurotransmitter transporters, and metal ion transporters (Nelson et al., 2002). Alternatively, a small NBC-mediated conductance (e.g., HCO_3^-) that is independent of Na^+-coupled transport may be responsible. A Na^+ conductance has been described for the electroneutral NBC, NBCn1 (Choi et al., 2000).

We used data from experiments similar to that shown in Fig. 7 A to determine the Na^+ dependencies of NBCe1-A, -B, and -C. For each experiment, we normalized the current elicited by 5% CO_2/33 mM HCO_3^- solutions containing different [Na^+]s to the mean current elicited by a flanking CO_2/HCO_3^- solution containing full, 98.5 mM Na^+. HCO_3^- currents obtained in the absence of Na^+ were subtracted before normalization. We plot the external Na^+ dependencies for the two most dissimilar variants: NBCe1-A in Fig. 7 C and NBCe1-C in Fig. 7 D. The apparent K_m and normalized V_{max} values are similar for both the A and C variants. The apparent K_M values are 20.6 ± 1.7 mM for NBCe1-A ($n = 33$ from five oocytes) and 31.7 ± 2.6 mM for NBCe1-C ($n = 71$ from 12 oocytes). Sciortino and Romero (1999) reported a similar apparent K_M of 30 mM for NBCe1-A. Our corresponding normalized V_{max} values are 1.21 ± 0.03 for NBCe1-A and 1.31 ± 0.04 for NBCe1-C. In additional studies, we also examined the external Na^+ dependence of NBCe1-B and obtained an apparent K_M of 35.5 ± 3.7 mM and normalized V_{max} of 1.35 ± 0.05 ($n = 23$ from five oocytes). In conclusion, all three NBCe1 variants have similar external Na^+ dependencies.

Role of the Amino Termini on the Function and Expression of NBCe1 Variants in Oocytes

According to the aforementioned HCO_3^- and Na^+ dependence data, the higher NBC current seen with NBCe1-A vs. -B and -C (Figs. 4 and 5) is not due to

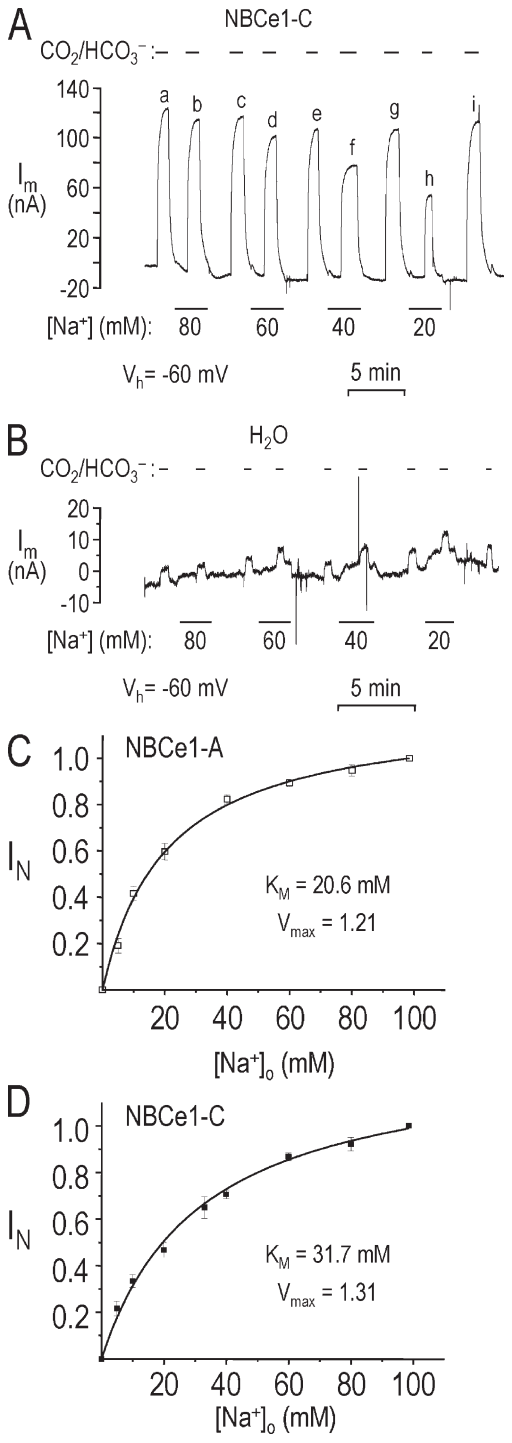

Figure 7. External Na^+ dependencies of NBCe1-A and -C. (A) A voltage-clamped oocyte (V_h = −60 mV) expressing NBCe1-C was exposed to 5% CO_2/33 mM HCO_3^- solutions containing different [Na^+]s. (B) The experimental protocol used in A was performed on an H_2O-injected oocyte. (C) Normalized HCO_3^--induced currents as a function of external [Na^+] for oocytes expressing NBCe1-A (r^2 = 0.98). HCO_3^--induced outward currents at different Na^+ concentrations were normalized to the mean currents elicited by the flanking exposures to the 33 mM HCO_3^- solution containing "full" 98.5 mM Na^+. (D) Normalized HCO_3^--induced currents as a function of external [Na^+] for oocytes expressing NBCe1-C (r^2 = 0.97).

higher substrate affinities. Therefore, the A variant must have a higher transport velocity compared to the B and C variants. As shown in Fig. 1, the differences in amino acid sequence among these three variants reside only at the amino and/or carboxy termini. The amino terminus is likely responsible for differences in NBC activity because the B and C variants (with low activity) share the same amino terminus, which is different than the unique amino terminus of the A variant (with high activity). Furthermore, the A/C chimera containing the unique carboxy terminus of C attached to the A variant displays NBC currents similar to those of the wild-type A variant.

Activity and Surface Expression of NBCe1 Variants Truncated before the First Transmembrane Domain. We used the HCO_3^--induced, outward-current assay shown in Fig. 5 A to examine the function of NBCe1 constructs with amino-terminal truncations. The three experimental traces shown in Fig. 8 A are from voltage-clamped oocytes injected with cRNA encoding wild-type NBCe1-C (C_{WT}), NBCe1-C missing the first 426 residues before the first predicted transmembrane domain ($C_{\Delta N426}$), or NBCe1-C missing the first 213 residues ($C_{\Delta N213}$). Oocytes exposed to a solution containing 5% CO_2/33 mM HCO_3^- elicited an outward current of ~250 nA in the oocyte expressing C_{WT}, but little/no current in the oocyte expressing either $C_{\Delta N426}$ or $C_{\Delta N213}$.

From experiments similar to those shown in A, the mean CO_2/HCO_3^--induced currents from oocytes expressing $C_{\Delta N426}$ or $C_{\Delta N213}$ were similar to those seen in day-matched, H_2O-injected oocytes, and more than 90% less than those in day-matched, C_{WT}-expressing eggs (Fig. 8 B). (Because we often examined several constructs on a given day, we necessarily used current and SOC data obtained from oocytes injected with H_2O and/or wild-type NBC constructs in more than one analysis.) A similar loss of NBC activity was observed with the homologous truncation of NBCe1-A before the first transmembrane domain, $A_{\Delta N382}$ (n = 2, not depicted).

SOC analysis was performed on the same two oocyte batches, and luminescence for each oocyte was normalized to the mean luminescence of oocytes expressing wild-type C_{WT}. Compared with the mean Norm. Lum. for C_{WT}, the mean values were actually 50% higher (P = 0.002) for $C_{\Delta N426}$ and similar (P = 0.14) for $C_{\Delta N213}$ (Fig. 8 C). In summary, the lost NBC activity of $C_{\Delta N426}$ and $C_{\Delta N213}$ is not due to the absence of expression at the plasma membrane.

In further structure–function studies, we examined the effects on transporter activity and plasma membrane expression of removing the NH_2-terminal 43 residues of NBCe1-A ($A_{\Delta N43}$) and 87 residues of NBCe1-C ($C_{\Delta N87}$). Because the amino terminus of the B and C variants is identical, studies on $C_{\Delta N87}$ provide NH_2-terminal information on the B variant.

Activity and Surface Expression of NBCe1-A Lacking its Unique Amino Terminus. At a holding potential of –60 mV, an oocyte expressing $A_{\Delta N43}$ (Fig. 9 A, left) displayed an HCO_3^--induced outward current that was ~50% smaller than the current seen in the oocyte expressing wild-type NBCe1-A (A_{WT}). Therefore, removing the amino-terminal 43 residues of the A variant decreases transporter activity. The summary data of HCO_3^--mediated outward currents are shown in Fig. 9 B (left). From five batches of oocytes, the mean HCO_3^--induced current for $A_{\Delta N43}$ (443 ± 31 nA, $n = 18$) was 55% smaller ($P < 0.001$) than the mean current for A_{WT} (990 ± 81 nA, $n = 15$). The mean HCO_3^--induced current from batch-matched, H_2O-injected oocytes was only 0.8% of the mean current from A_{WT}-expressing oocytes.

In four of these five batches in which SOC data were obtained, the mean Norm. Lum. was 10% lower (marginal significance; $P = 0.05$) for oocytes injected with $A_{\Delta N43}$ compared to those injected with A_{WT} (Fig. 9 C, left). A 10% lower surface expression would not explain the 55% decrease in transporter activity of $A_{\Delta N43}$ compared to A_{WT}. In addition, in one of these four batches in which the surface expression of $A_{\Delta N43}$ ($n = 5$) was 96 ± 14% of A_{WT} ($n = 5$), the mean NBC- mediated current for $A_{\Delta N43}$ (656 ± 105 nA, $n = 3$) was 46% smaller ($P = 0.04$) than for A_{WT} (1220 ± 192 nA, $n = 3$). Therefore, the lower activity of $A_{\Delta N43}$ compared to A_{WT} cannot be explained by a difference in surface expression.

Activity and Surface Expression of NBCe1-C Lacking the Different Amino Terminus. Different results were obtained with the homologous NH_2-terminal truncation of NBCe1-C ($C_{\Delta N87}$). At a holding potential of –60 mV, an oocyte expressing $C_{\Delta N87}$ (Fig. 9 A, right) displayed an HCO_3^--induced outward current that was 3.4-fold larger than the current seen in the oocyte expressing C_{WT}. Therefore, removing the amino-terminal 87 residues of C_{WT} increases transporter activity. The summary data of HCO_3^--mediated outward currents from experiments similar to those shown in Fig. 9 A (right) are shown in B (right). From seven batches of oocytes, the mean HCO_3^--induced current for $C_{\Delta N87}$ (654 ± 48 nA, $n = 23$) was 2.7-fold larger ($P < 0.001$) than the mean current for C_{WT} (242 ± 12 nA, $n = 19$). As expected from Fig. 5 data, the mean current for C_{WT} was ~25% of the mean current for A_{WT}.

In five of the seven batches above in which SOC data were obtained, the mean Norm. Lum. was 33% higher ($P < 0.001$) for oocytes injected with $C_{\Delta N87}$ compared to those injected with C_{WT} (Fig. 9 C, right). A 33% increase in surface expression would not explain the 170% increase in transporter activity of $C_{\Delta N87}$ compared with C_{WT}. Moreover, in two of these five batches in which the surface expression of $C_{\Delta N87}$ ($n = 9$) was 102 ± 4% of C_{WT} ($n = 10$), the mean NBC-mediated current for $C_{\Delta N87}$ (713 ± 137 nA, $n = 6$) was also 2.7- fold larger ($P = 0.01$) than for C_{WT} (264 ± 20 nA, $n = 5$). Therefore, the higher activity of $C_{\Delta N87}$ compared to C_{WT} cannot be explained by a difference in surface expression. Data from Fig. 9 are consistent with the amino-terminal residues of NBCe1-A stimulating transporter activity, and the amino-terminal residues of NBCe1-B and C inhibiting transporter activity.

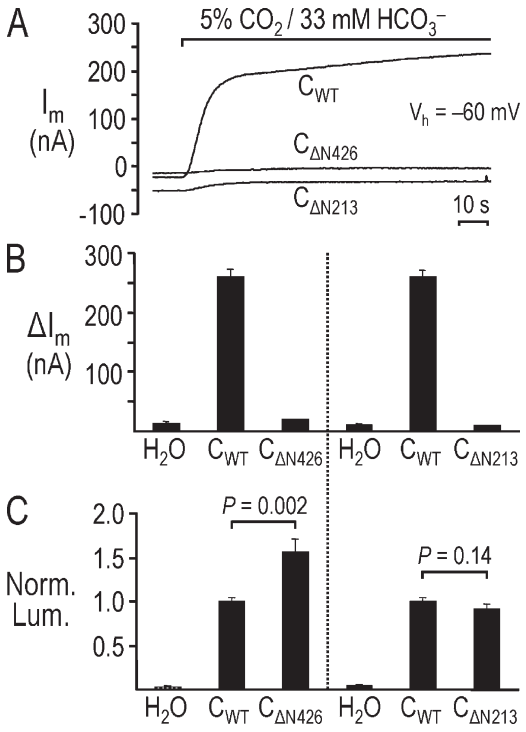

Figure 8. Inhibited NBCe1 activity elicited by removing regions of the cytosolic amino terminus. (A) Exposing oocytes to a solution containing 5% CO_2/33 mM HCO_3^- elicited an outward current in the oocyte expressing wild-type NBCe1-C (C_{WT}), but little/no current in the oocyte expressing either $C_{\Delta N426}$ or $C_{\Delta N213}$. (B) Summary of HCO_3^--induced outward currents from experiments similar to those shown in A. For each bar, $n \geq 3$ from two batches of oocytes. SEM values for the $C_{\Delta N426}$ or $C_{\Delta N213}$ data are small. (C) Compared to the mean normalized luminescence (Norm. Lum.) for C_{WT}, mean Norm. Lum. was 1.5-fold greater for $C_{\Delta N426}$, and similar for $C_{\Delta N213}$ in oocytes from the same two batches in B. $n \geq 10$ for each bar.

If the amino termini of the NBCe1 variants are solely responsible for the higher transporter activity seen with A compared to B and C, then the activities of $A_{\Delta N43}$ and $C_{\Delta N87}$ should be identical. However, as shown in Fig. 9, the mean $C_{\Delta N87}$ current (654 nA) is ~50% larger ($P < 0.001$) than the mean $A_{\Delta N43}$ current (443 nA). The larger mean $C_{\Delta N87}$ current could be explained by the slightly higher surface expression of $C_{\Delta N87}$ vs. $A_{\Delta N43}$ as revealed in the SOC analysis shown in Fig. 9 C. However, a difference in surface expression does not appear to be the only explanation according to current–voltage (I-V) analyses (Fig. 10).

I-V Relationships of Wild-type and Mutant NBCe1-A and C Constructs. We next examined the I-V relationships of

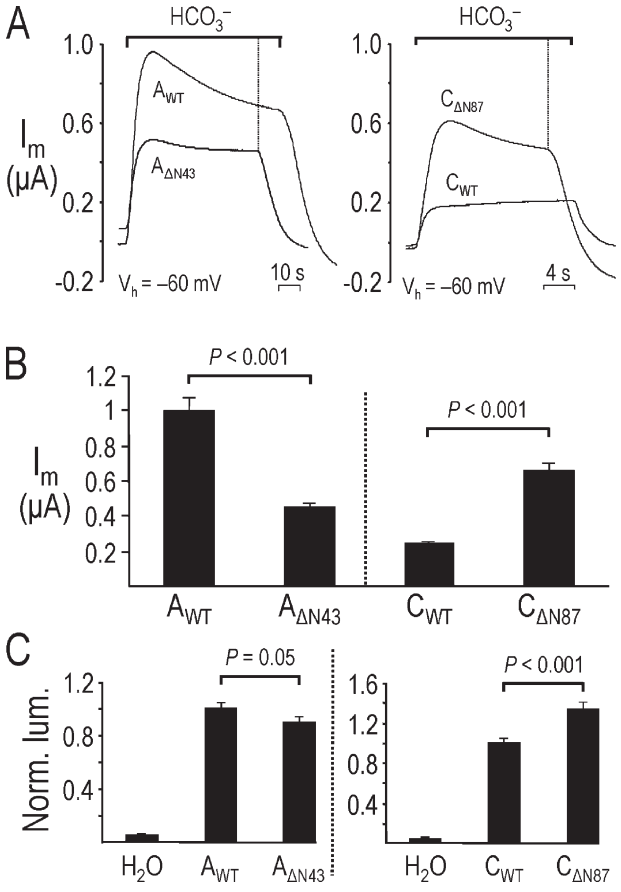

Figure 9. Changes in NBCe1 activity elicited by removing the different amino termini. (A, left) An oocyte expressing mutant $A_{\Delta N43}$ displayed a peak HCO_3^--induced outward current that was ~50% smaller than seen in the oocyte expressing A_{WT}. (A, right) An oocyte expressing mutant $C_{\Delta N87}$ displayed a peak HCO_3^--induced outward current that was approximately threefold larger than seen in the oocyte expressing C_{WT}. (B) Summary of HCO_3^--induced outward currents from experiments similar to those shown in A. $n \geq 15$ for each bar. (C, left) The mean normalized luminescence (Norm. Lum.) was 10% lower for $A_{\Delta N43}$ compared with A_{WT}. $n \geq 19$ for each bar. (C, right) The mean Norm. Lum. was 33% higher for $C_{\Delta N87}$ compared with C_{WT}. $n \geq 23$ for each bar.

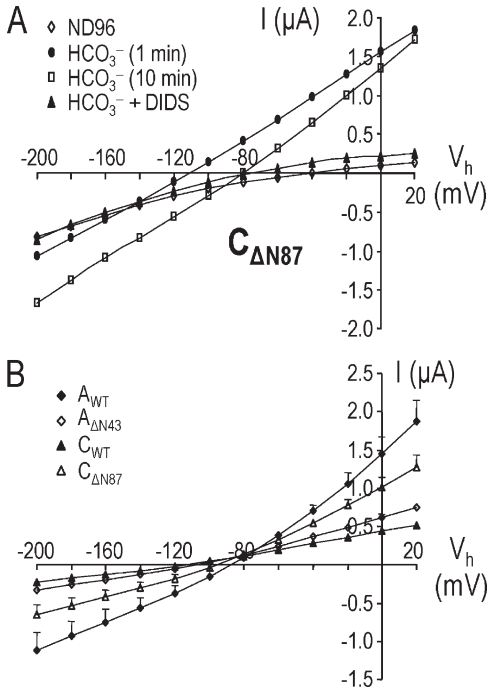

Figure 10. Current–voltage (I-V) relationships from oocytes expressing wild-type and amino-terminal truncations of NBCe1 variants. (A) Representative experiment on an oocyte expressing $C_{\Delta N87}$ in which I-V plots were obtained with the oocyte initially bathed in ND96 (diamonds), followed by 1 min in 5% CO_2/33 mM HCO_3^- (circles) and then 10 min in the physiological buffer (squares), and finally in the HCO_3^- solution containing 200 μM DIDS (triangles). (*B*) HCO_3^--dependent I-V plots for NBCe1-A (closed diamonds), $A_{\Delta N43}$ (open diamonds), NBCe1-C (closed triangles), and $C_{\Delta N87}$ (open triangles). Data were obtained from experiments similar to that shown in A. $n = 3$ for each data point from a single batch of oocytes. SEM bars smaller than symbol sizes are not shown. Similar results were obtained from a second batch of oocytes.

A_{WT}, C_{WT}, $A_{\Delta N43}$, and $C_{\Delta N87}$. A representative experiment on an oocyte expressing $C_{\Delta N87}$ is shown in Fig. 10 A. I-V relationships were obtained from the oocyte first bathed in ND96 (diamonds), then after 1 min (circles) and 10 min (squares) in 5% CO_2/33 mM HCO_3^-, and finally after 2 min in the physiological buffer containing 200 μM DIDS (triangles). The larger currents obtained with the oocyte in CO_2/HCO_3^- were inhibited by the presence of 200 μM DIDS. The left-shifted I-V plot obtained after a 1 vs. 10 min exposure to CO_2/HCO_3^- was due to the incomplete equilibration of CO_2/HCO_3^- across the membrane, and consequently, a larger extracellular-to-intracellular HCO_3^- gradient.

From experiments similar to that shown in Fig. 10 A, mean HCO_3^--dependent I-V plots were obtained from oocytes injected with wild-type NBCe1-A and -C, and the truncated constructs $A_{\Delta N43}$ and $C_{\Delta N87}$ (Fig. 10 B). The data were from day-matched experiments, and mean I-V data from H_2O-injected oocytes were subtracted. Similar to the Fig. 9 results obtained at a fixed potential of −60 mV, the voltage-dependent $A_{\Delta N43}$ currents (Fig. 10 B, open diamonds) were smaller than the corresponding wild-type A currents (closed diamonds), and the $C_{\Delta N87}$ currents (open triangles) were larger than the corresponding wild-type C currents (closed triangles) at all holding potentials from −200 to +20 mV (except at −80 mV). For each construct, the NBC conductance (g_{NBC}) was determined from the slope of a linear fit to either the mean inward currents (V_h from −200 to −100 mV), or the mean outward currents (V_h from −80 to +20 mV) plotted in Fig. 10 B. For the inward currents, the g_{NBC} of $A_{\Delta N43}$ was 64% lower than that of A_{WT}, and the g_{NBC} of $C_{\Delta N87}$ was 2.3-fold higher than that of C_{WT}. Expectedly, the g_{NBC} of C_{WT} was only 28% of the g_{NBC} of A_{WT}. Similar g_{NBC} results were obtained for the outward currents.

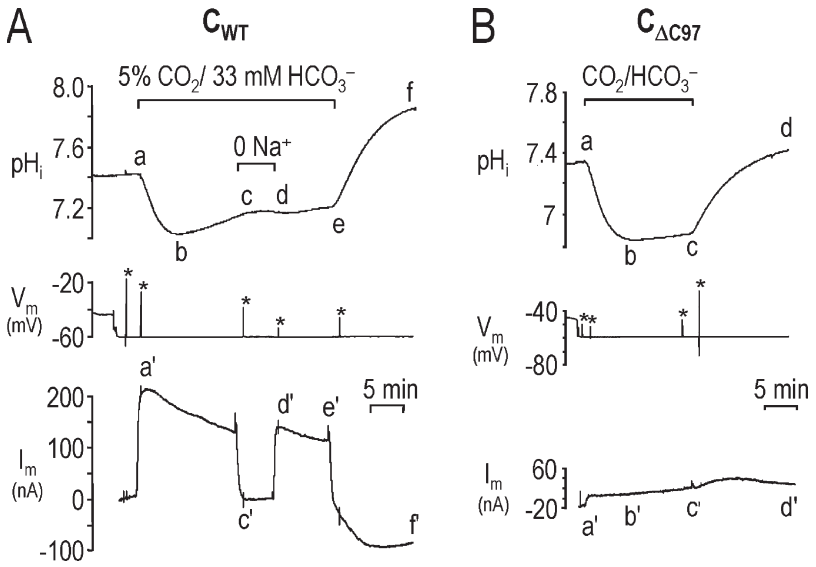

Figure 11. Lost activity of $C_{\Delta C97}$ expressed in oocytes. (A) pH_i (top trace), voltage (middle trace), and current (bottom trace) were measured simultaneously in an NBCe1-C–injected oocyte that was initially bathed in ND96. The oocyte was then voltage clamped and exposed to a solution containing 5% CO_2/33 mM HCO_3^- during segment ae. Electrogenic NBC activity was evident from the instantaneous outward current (a'), and the pH_i recovery (bc) following the initial CO_2-induced acidification (ab). Removing Na^+ blocked the pH_i recovery (cd), and reversed the hyperpolarization (c'). (B) The same experimental protocol in A was performed on a $C_{\Delta C97}$-injected oocyte. Exposing the oocyte to CO_2/HCO_3^- elicited only a small outward current (a'), and minimal pH_i recovery (bc) following the initial decrease in pH_i (ab).

$C_{\Delta N87}$ currents were also found to be consistently larger than the $A_{\Delta N43}$ currents. The mean $C_{\Delta N87}$ current was approximately twofold larger than the mean $A_{\Delta N43}$ current at −200 and +20 mV. Furthermore, g_{NBC} of $C_{\Delta N87}$ was 1.8-fold higher than the g_{NBC} of $A_{\Delta N43}$. These data are consistent with the unique carboxy terminus of the C variant vs. the carboxy terminus of the A/B variant contributing to higher NBC activity in the absence of the amino terminus.

Role of the Carboxy Termini on the Function and Expression of NBCe1 Variants in Oocytes

Activity and Surface Expression of NBCe1 Truncated after the Last Transmembrane Domain. To determine the importance of the cytosolic carboxy terminus of NBCe1, we removed the 97 residues after the last predicted transmembrane domain of NBCe1-C ($C_{\Delta C97}$). This construct is identical to the homologous truncation of NBCe1-B. After expressing $C_{\Delta C97}$ in oocytes, we used pH-sensitive microelectrodes and the voltage-clamp technique to measure simultaneously pH_i and membrane current of oocytes voltage clamped at −60 mV.

Records from simultaneous pH_i and voltage-clamp experiments on oocytes expressing wild-type NBCe1-C (C_{WT}) and $C_{\Delta C97}$ are shown in Fig. 11. After stable pH_i and V_m values were obtained, oocytes were voltage clamped at −60 mV and exposed to 5% CO_2/33 mM HCO_3^-. As expected from Fig. 2 and Fig. 5 data, the C_{WT}-expressing oocyte (panel A) exhibited an instantaneous HCO_3^--stimulated outward current (point a′, bottom trace), as well as a pH_i recovery following the initial CO_2-induced acidification (abc, top trace). Removing external Na^+ reversed the outward current (c′), and blocked the pH_i recovery (cd). In contrast, the $C_{\Delta C97}$-expressing oocyte (panel B) exposed to CO_2/HCO_3^- exhibited neither a HCO_3^--stimulated outward current (point a′, bottom trace), nor any appreciable pH_i recovery after the CO_2-induced acidification (abc, upper trace). Stars in the voltage traces represent time points during the experiment when I-V plots were obtained (unpublished data).

The summary data from experiments similar to those shown in Fig. 11 (A and B) are shown in Fig. 12 (A and B). Data were obtained from two batches of oocytes. The mean rate of pH_i recovery (dpH_i/dt) during the segment bc pH_i recovery in oocytes expressing $C_{\Delta C97}$ was fourfold less than the pH_i recovery rate in oocytes expressing C_{WT}, and similar ($P > 0.14$) to the rate in oocytes injected with H_2O (panel A). The mean CO_2/HCO_3^--induced outward current (a′) was 14-fold smaller in oocytes expressing $C_{\Delta C97}$ compared to C_{WT}, and no different ($P > 0.18$) than the mean current in H_2O-injected eggs (panel B).

To identify the explanation for the lost transporter activity of $C_{\Delta C97}$, we used immunoblotting and SOC techniques to examine protein expression. According to the immunoblot data shown in Fig. 12 C, a polyclonal antibody to the amino terminus of NBCe1 recognized the expected-size protein from total microsomal protein isolated from an oocyte injected with either $C_{\Delta C97}$ (lane 1) or C_{WT} (lane 3). No labeling was observed in protein from an H_2O-injected oocyte (lane 2). Thus, the injected $C_{\Delta C97}$ cRNA is translated and the protein is expressed in a microsomal fraction. However, according to the SOC data (normalized to the mean luminescence of C_{WT}-expressing oocytes), the normalized mean luminescence of $C_{\Delta C97}$-injected oocytes is approximately threefold lower than that of C_{WT}, and even slightly lower than that of H_2O-injected oocytes ($P < 0.01$). Therefore, $C_{\Delta C97}$ is not expressed at the plasma membrane of oocytes, a result that was confirmed by immunocytochemistry with the anti-HA antibody

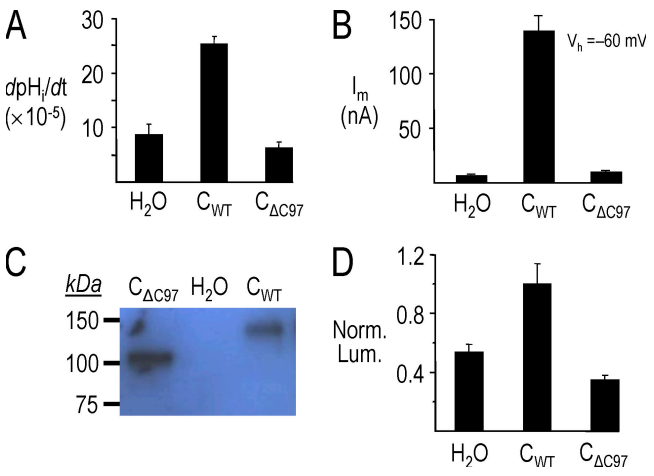

Figure 12. Lost activity of $C_{\Delta C97}$ expressed in oocytes due to poor expression at the plasma membrane. (A) Summary data of the segment-bc pH_i recovery rates from experiments similar to those shown in Fig. 11, top traces. $n \geq 4$ for each bar. (B) Summary of H_2O-subtraced, HCO_3^--induced currents from experiments similar to those shown in Fig. 11, bottom traces. For each bar, $n \geq 6$ from two batches. (C) Immunoblot analysis of total microsomal protein from single oocytes injected with H_2O, $C_{\Delta C97}$ cRNA, and C_{WT} cRNA. An NBCe1 antibody labeled bands of the expected sizes: ~130 kD for C_{WT} and ~118 kD for $C_{\Delta C97}$. No labeling was observed in protein from an H_2O-injected oocyte. (D) The mean normalized luminescence (Norm. Lum.) for oocytes injected with $C_{\Delta C97}$ and H_2O are similar. $n \geq 10$ from two batches of oocyte.

(unpublished data). In summary, the loss of $C_{\Delta C97}$ activity in oocytes is due to the absence of $C_{\Delta C97}$ protein at the plasma membrane.

Activity and Surface Expression of NBCe1 Variants Truncated at the Different Carboxy Termini. To explore the contribution of the different carboxy termini of the NBCe1 variants to plasma membrane expression, and possibly function, we performed additional studies comparing the expression and function of wild-type and truncated variants. More specifically, we created two additional constructs: NBCe1-A truncated 46 residues from the carboxy terminus ($A_{\Delta C46}$) and NBCe1-C truncated 61 residues from the carboxy terminus ($C_{\Delta C61}$). The $C_{\Delta C61}$ construct is identical to the homologous truncation of NBCe1-B.

NBC-mediated outward currents in response to CO_2/HCO_3^- are shown in Fig. 13 A for two voltage-clamped oocytes; one expressing A_{WT} and the other expressing $A_{\Delta C46}$. The HCO_3^--induced outward current of ~0.43 μA in the $A_{\Delta C46}$-expressing oocyte was 71% smaller than the current of ~1.45 μA in the A_{WT}-expressing oocyte. The summary data from similar experiments performed on A_{wt} and $A_{\Delta C46}$, as well as C_{wt} and $C_{\Delta C61}$ are plotted in Fig. 13 B. The mean currents obtained from H_2O-injected oocytes were subtracted from the corresponding currents seen in the NBC-injected oocytes. The mean NBC-mediated currents of the truncated NBCs were ~30% of the corresponding wild-type NBCs. As shown in Fig. 13 C, both A_{WT} and $A_{\Delta C46}$ are expressed in a microsomal membrane fraction. Similar results were obtained with C_{WT} and $C_{\Delta C61}$ (not depicted). However, according to summary SOC data (Fig. 13 D) from the same batches of oocytes, $A_{\Delta C46}$ and $C_{\Delta C61}$ are poorly expressed at the plasma membrane compared to the corresponding wild-type NBCs. Therefore, the reduced activity of $A_{\Delta C46}$ and $C_{\Delta C61}$ in oocytes is predominantly due to low surface expression.

Transporter Activity of NBCe1 Variants in the Inside-out Macropatch

To examine the contribution of the amino termini to NBCe1 transporter activity in the absence of cytosolic factors, we next examined the function of C_{WT}, A_{WT}, $C_{\Delta N87}$, and $A_{\Delta N43}$ in excised macropatches in the inside-out configuration from oocytes. In our experimental protocol (Fig. 14 A), we excised patches into a low-Cl^- (2 mM), ND96 solution and then activated NBCs by exposing the patch to the low-Cl^- solution containing 5% CO_2/33 mM HCO_3^-. NBC-mediated inward currents were obtained at a holding pipette potential (V_p or $-V_m$) of +60 mV.

C_{WT} and $C_{\Delta N87}$. As shown in Fig. 14 B, there was no appreciable change in current when a macropatch from an H_2O-injected oocyte was exposed first to CO_2/HCO_3^-, and then to the HCO_3^- solution containing 200 μM DIDS. In contrast, exposing a macropatch from a C_{WT}-expressing oocyte to CO_2/HCO_3^- elicited an inward current of ~5 pA (Fig. 14 C). This inward current is consistent with NBC- mediated net-negative charge moving from the bath to the pipette held at +60 mV. Switching back to the ND96 solution caused the current to return to the original level. In many experiments with either the C or A variant, we could reactivate this HCO_3^--induced inward current by reexposing the patch to the CO_2/HCO_3^- solution (unpublished data). However, the current change elicited by the second HCO_3^- exposure was often smaller—a result consistent with "rundown" of transporter activity. The phenomenon of rundown is observed with channels such as ROMK1 (McNicholas et al., 1994), and reflects events such as protein dephosphorylation (McNicholas et al., 1994) or loss of protein interaction with membrane phospholipids such as phosphatidylinositol 4,5-bisphosphate (PIP_2) (Huang et al., 1998; Suh and Hille, 2005).

As shown in Fig. 14 D, exposing a macropatch from an oocyte expressing $C_{\Delta N87}$ to the low-Cl^-, CO_2/HCO_3^- solution elicited a large inward current of ~28 pA. The current was ~5.5-fold larger than the HCO_3^--induced current seen with C_{WT} (Fig. 14 C). If these HCO_3^--induced inward currents are NBC mediated, then they should be inhibited by stilbene derivatives such as DIDS. Indeed, the inward current seen with $C_{\Delta N87}$ was

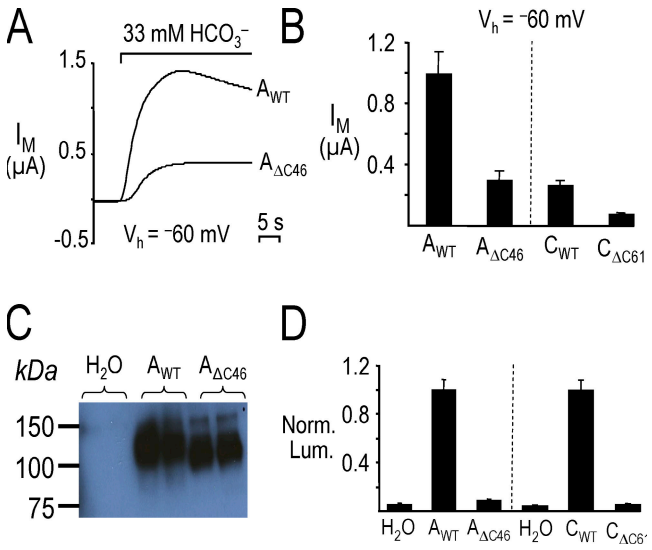

Figure 13. Reduced activity and low surface expression of $A_{\Delta C46}$ and $C_{\Delta C61}$ expressed in oocytes. (A) 5% CO_2/33 mM HCO_3^- elicited an outward current in an oocyte expressing NBCe1-A (A_{WT}) that was markedly larger than the current in the oocyte expressing $A_{\Delta C46}$. (B) Summary of H_2O-subtracted, HCO_3^--induced currents from experiments similar to those shown in A. $n \geq 6$ for each bar from two batches of oocytes. (C) Immunoblot analysis of total microsomal protein from single oocytes injected with H_2O, A_{WT} cRNA, or $A_{\Delta C46}$ cRNA. An NBCe1 antibody labeled bands of the expected sizes: ~130 kD for A_{WT} and ~120 kD for $A_{\Delta C46}$. (D) The mean normalized luminescence (Norm. Lum.) for oocytes expressing the truncated NBCs were markedly less than the Norm. Lum. for oocytes expressing the corresponding wild-type NBCs. $n \geq 11$ for each bar from two batches of oocytes.

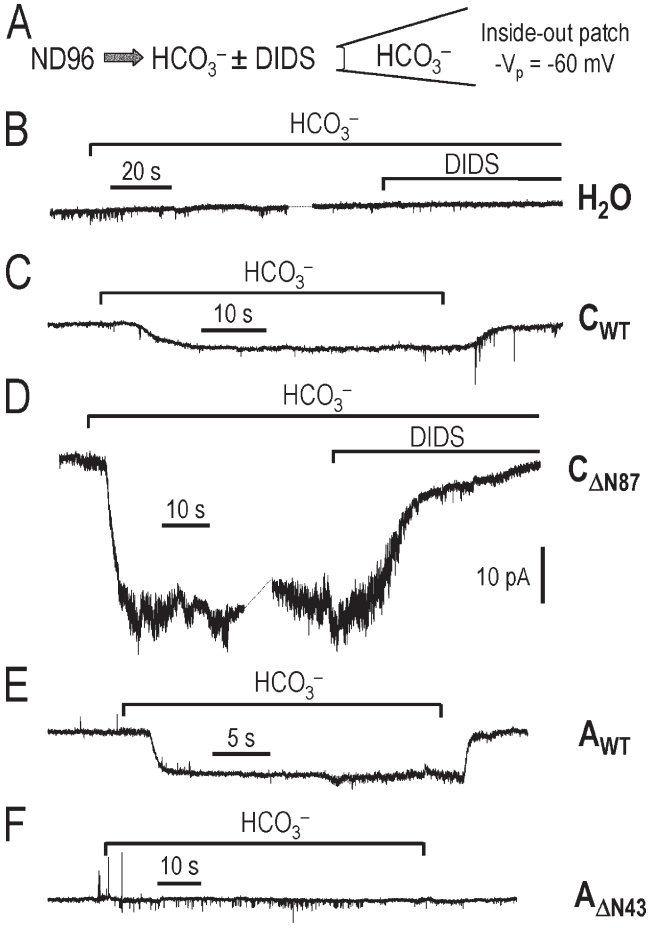

Figure 14. NBCe1 activity from inside-out macropatches excised from oocytes. (A) NBC-mediated inward currents were elicited by exposing patches to a low-Cl^-, 5% CO_2/33 mM HCO_3^- solution ± 200 μM DIDS with the patch pipette ($-V_p = -60$ mV) containing the same low-Cl^-, 33 mM HCO_3^- solution. (B) H_2O-injected oocyte. The HCO_3^- solution without or with DIDS did not elicit any change in current. (C) C_{WT}-injected oocyte. The HCO_3^- solution elicited a small inward current that was reversible when the patch was returned to ND96. (D) $C_{\Delta N87}$-injected oocyte. The inward current elicited by the HCO_3^- solution was larger than the current seen in C, and completely inhibited by DIDS. (E) A_{WT}-injected oocyte. The HCO_3^- solution elicited a small, reversible inward current. (F) $A_{\Delta N43}$-injected oocyte. No change in current was observed when the patch was exposed to HCO_3^-.

completely reversed by exposing the patch to 200 μM DIDS in the continued presence of CO_2/HCO_3^- (Fig. 14 D). DIDS inhibits NBCe1 activity from either the extracellular or intracellular side of an oocyte macropatch (Heyer et al., 1999). In a total of five experiments similar to that shown in D, the mean HCO_3^--induced inward current was inhibited 89 ± 11% by 200 μM DIDS. The mean HCO_3^--induced inward current seen with C_{WT} (e.g., in Fig. 14 C) was also inhibited 103 ± 30% ($n = 3$) by DIDS. In summary, the larger HCO_3^--stimulated currents elicited by removing the amino terminus of NBCe1-C reported above in the whole-cell experiments (Figs. 9 and 10) are also seen in macropatches excised from the oocyte.

A_{WT} and $A_{\Delta N43}$. We performed macropatch experiments on A_{WT} and $A_{\Delta N43}$ using the aforementioned protocol. Based on the finding that macropatch currents for $C_{\Delta N87}$ were larger than those of C_{WT}, an observation that paralleled the whole-cell data, we anticipated A_{WT} to exhibit the largest macropatch currents of all the NBC constructs in the present study. As shown in Fig. 14 E, an HCO_3^--induced, NBC-mediated current of ~7 pA was indeed obtained in a macropatch from an oocyte expressing A_{WT}. Unexpectedly however, the mean A_{WT} current was of similar magnitude to the C_{WT} current (Fig. 14 C), and considerably less than the $C_{\Delta N87}$ current (D). In additional studies (not depicted), we confirmed that this A_{WT}-mediated HCO_3^--induced current was eliminated with 200 μM DIDS. The inward current elicited by CO_2/HCO_3^- in a macropatch expressing $A_{\Delta N43}$ was absent (Fig. 14 F). The NBC-mediated current rose much faster for the A_{WT} (Fig. 14 E) variant than the C_{WT} variant (C)—an observation also made in whole-cell experiments (see Fig. 5). Therefore, the activation kinetics of A appear faster than those of C, even in the absence of the cytosol.

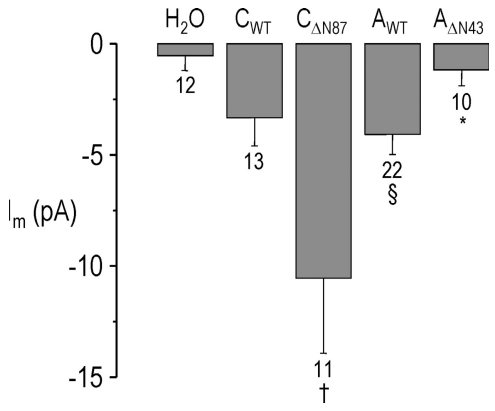

Figure 15. Summary macropatch data from experiments similar to those shown in Fig. 14 on oocytes injected with H_2O, C_{WT}, $C_{\Delta N87}$, A_{WT}, and $A_{\Delta N43}$. The mean HCO_3^--induced macropatch current for $C_{\Delta N87}$ is 3.2-fold larger than the mean current for C_{WT} (†, $P = 0.03$). The mean HCO_3^--induced currents for A_{WT} and C_{WT} are similar (§, $P = 0.32$), and both are larger than the mean current seen in H_2O-injected oocytes ($P < 0.05$). The mean current for $A_{\Delta N43}$ is 71% smaller than that of A_{WT} (*, $P < 0.01$). *n* values are shown under bars.

From experiments similar to those shown in Fig. 14 (B–F), we plotted the mean HCO_3^--induced currents from a total of 68 inside-out macropatch experiments (Fig. 15). Similar to the results from the whole-cell data, the mean macropatch current for $C_{\Delta N87}$ is 3.2-fold larger than the mean current for C_{WT} ($P = 0.03$), whereas the mean current for $A_{\Delta N43}$ is 71% less than that of A_{WT} ($P < 0.01$). In fact, the mean macropatch currents from oocytes injected with $A_{\Delta N43}$ and H_2O are indistinguishable ($P = 0.25$). Macropatch data in disagreement with the whole-cell data include the absence of $A_{\Delta N43}$ current, as well as similar mean currents for A_{WT} and C_{WT} ($P = 0.32$). These disagreements may reflect the absence of a cytosolic component in the macropatch experiments that is necessary for both the $A_{\Delta N43}$ current and the large A_{WT} current seen in the whole-cell experiments.

DISCUSSION

Activity of NBCe1 Variants

In this study, we compared the function and expression of the three NBCe1 variants (A, B, and C) heterologously expressed in *Xenopus* oocytes. In whole-cell experiments, the A variant displayed larger NBC currents than the B and C variants; an observation not due to differences in plasma membrane expression, or differences in voltage or external ion dependencies. The higher transport velocity of the A variant is due to its unique amino terminus. In both whole-cell and macropatch studies, removing the unique amino terminus of the A variant decreases activity, whereas removing the different amino terminus of the C variant increases activity.

Voltage and Ion Dependencies of NBCe1 Variants in *Xenopus* Oocytes

While all three variants exhibited similar voltage and external ion dependencies, the reversal potential (E_{rev}) of NBCe1-A was more positive (~−85 mV) than the E_{rev} values of the B and C variants (~−160 mV) (Fig. 4 A). Working on rat kidney NBCe1-A expressed in oocytes, Sciortino and Romero (1999) obtained an E_{rev} similar to ours, and calculated a corresponding 1:2 Na^+:HCO_3^- stoichiometry for the transporter. As mentioned in Results, the more negative E_{rev} values for the B and C variants are unlikely to reflect different Na^+:HCO_3^- stoichiometries; but rather, different substrate and pH gradients established immediately across the plasma membrane by the variants. Indeed, we observed a similar negative shift of E_{rev} in oocytes displaying smaller NBCe1-A currents in response to less cRNA injected (Fig. 4 B). Furthermore, the I-V relationships for the three variants looked similar when we adjusted expression levels and matched the magnitude of the whole-cell, transporter currents (Fig. 4 C).

For the NBCe1 variants, we calculated transporter stoichiometry using E_{rev} values and the extracellular Na^+ and HCO_3^- concentrations used in the study. The equilibrium potential of an electrogenic NBC (E_{NBC}) is described by the following equation (Boron and Boulpaep, 1983; Deitmer and Schlue, 1989):

$$E_{NBC} = \frac{RT}{(n-1)F} \ln \frac{[Na^+]_i [HCO_3^-]_i^n}{[Na^+]_o [HCO_3^-]_o^n}, \quad (1)$$

where *R*, *T*, and *F* have their usual meanings, and *n* is the HCO_3^-:Na^+ stoichiometry. Solving Eq. 1 for *n* yields the transformed equation:

$$n = \frac{E_{NBC}F - RT \ln x}{E_{NBC}F + RT \ln y}, \quad (2)$$

$$\text{where} \quad x = \frac{[Na^+]_o}{[Na^+]_i} \quad \text{and} \quad y = \frac{[HCO_3^-]_o}{[HCO_3^-]_i}.$$

We determined the mean intracellular HCO_3^- concentration of ~8.3 mM from simultaneous pH_i and voltage-clamp experiments on NBCe1-C–expressing oocytes similar to those shown in Fig. 11 A. For the intracellular Na^+ concentration, we used a measured value of 10.4 mM previously reported by Sciortino and Romero (1999) for unclamped oocytes expressing NBCe1-A. Our calculated Na^+:HCO_3^- stoichiometries are 1:1.8 for the B variant and 1:1.7 for the C variant. These values are similar to the 1:2 Na^+:HCO_3^- stoichiometry previously calculated for the A variant (Sciortino and Romero, 1999). Moreover, we used the E_{rev} of −120/−140 mV from the I-V relationship shown in Fig. 4 (B and C) to calculate a similar Na^+:HCO_3^- stoichiometry of ~1:2 for the A variant. We used the lower-current I-V

relationships for the analysis to minimize the complication of a large NBC-mediated substrate/pH gradient across the membrane (see above). In summary, all three variants expressed in oocytes appear to have the same 1:2 Na^+:HCO_3^- stoichiometry.

Contribution of the Carboxy Termini to NBCe1 Activity

The carboxy-terminal truncations of NBCe1 variants examined in this study express poorly at the plasma membrane of oocytes. Based on our results, one or more regions within the different carboxy termini among the variants is/are required for proper plasma membrane expression in oocytes. Similarly, Cordat et al. (2003) reported that an AE1 construct truncated 11 residues from the carboxy terminus displayed reduced plasma membrane expression when expressed in HEK293 cells. Furthermore, Li et al. (2004) reported that GFP-tagged, human NBCe1-A mutants missing either the carboxy-terminal 26 or 50 residues retargets to the apical membrane of MDCK cells, and the latter construct displays significant intracytoplasmic expression. Our data with both $A_{\Delta C46}$ and $C_{\Delta C61}$ are consistent with this finding that the carboxy termini can influence trafficking. However, the effect of truncating the different carboxy termini found in A and C on plasma membrane expression is more dramatic in oocytes. The reduced surface expression could be due to the loss of a residue/region required for protein expression/stability, or an altered conformation that leads to organellar retention.

Contribution of the Amino Terminus to NBCe1 Activity

The following three general models would explain the contribution(s) of the different amino termini to NBC activity: (1) the unique amino terminus of A (A_{N41}) is stimulatory for an otherwise low-activity transporter, (2) the amino terminus of B/C is inhibitory (C_{N85}) for an otherwise high-activity transporter, or (3) both termini can influence function of an otherwise intermediate-activity transporter. Our observation that both whole-cell and macropatch NBC currents were inhibited to an intermediate level by $A_{\Delta N43}$ and stimulated to an intermediate level by $C_{\Delta N87}$ are consistent with the third possibility. The amino-terminal truncations likely lead to changes in transporter velocity. Indeed, the external Na^+ and HCO_3^- dependencies for $C_{\Delta N87}$ were similar to those for C_{WT} (unpublished data). Therefore, the different amino termini of the variants can influence transporter activity two to threefold even though they only comprise a small fraction of the entire NBCe1 sequence (4% for A and 8% for C). While the different amino termini stimulate or inhibit transporter activity, one or more regions of the cytosolic amino terminus downstream of the variable region are required for NBC function. Removing nearly all of the cytosolic amino terminus of NBCe1-A or -C, or approximately half of this region of NBCe1-C, leads to a complete loss of transporter function without affecting plasma membrane expression.

Potential Mechanism(s) for the Amino-terminal Effects. There are several possible mechanisms by which the amino terminus of an NBCe1 could affect transporter activity. An amino terminus may bind to a region of the same NBC protein and either elicit a change in protein conformation or directly interact with the ion translocation pathway. However, a specific carboxy terminus does not appear to be essential in light of the observation that the A variant and the A variant containing the carboxy terminus of C (A/C chimera) display a similar level of activity. Interaction with the translocation pathway may be similar to the "ball and chain" mechanism of inactivation of potassium channels (Zagotta et al., 1990; Tseng-Crank et al., 1993). Alternatively, the amino terminus of one NBC may exert its effect by binding to another NBC protein. Evidence for multimerization of NBCe1 has been reported in preliminary form (Espiritu, D.J.D., A.A. Bernardo, and J.A.L. Arruda. 2003. FASEB J. 17:A462; Espiritu, D.J.D., A.A. Bernardo, and J.A.L. Arruda. 2004. J. Am. Soc. Nephrol. 15:F-PO016.). Another mechanism for the amino-terminal effects may involve regulatory proteins/factors that are either cytosolic or membrane bound (see below). Regulatory proteins may serve as intermediate proteins that couple the amino termini to regions of an NBC protein.

NBCe1 Macropatch Currents

NBCe1-mediated HCO_3^- Transport across a patch of Oocyte Membrane. We used the macropatch technique in the inside-out configuration to examine the potential involvement of a cytosolic component on the activity of NBCe1 constructs expressed in oocytes. The magnitudes of our NBC macropatch currents were similar to those previously reported for rat NBCe1-A (Heyer et al., 1999). In our studies, it was not uncommon to record from patches with little or no NBC-mediated currents. For all NBC groups, there was a broad range of HCO_3^--mediated currents. For C_{WT}, current responses ranged from an outward current of 4.2 pA to an inward current of −14 pA. The range of responses may reflect different plasma membrane expression levels of NBCs among patches. Indeed, A_{WT} currents from three vegetal-pole patches obtained from each of two oocytes also exhibited a range of currents: 0.4, −5.1, and −3.3 pA for one oocyte, and −7.8, −3.3, and −7.4 pA for the other oocyte. NBCe1 expression at the oocyte surface may therefore be somewhat heterogeneous and reflect clustering of transporter proteins.

Influence of the Amino Termini on NBCe1 Activity. There are three noteworthy observations regarding the macropatch results and the influence of the amino termini on NBC activity. First, the mean macropatch current for

$C_{\Delta N87}$ is 3.2-fold larger than the mean current for C_{WT}. A similar 2.7-fold larger current for $C_{\Delta N87}$ was observed in the whole-cell experiments. Second, the mean current for $A_{\Delta N43}$ is less than that of A_{WT}. Similar results were obtained in the whole-cell experiments: the mean $A_{\Delta N43}$ current was 55% less than that of A_{WT}. Both of these observations corroborate the whole-cell data regarding the functional impact of the different amino termini.

The third observation in the macropatch studies, which deviates from the whole-cell data, is the observation that the mean macropatch current for A_{WT} is similar to the mean current for C_{WT}. Furthermore, the mean current for $A_{\Delta N43}$ is not only lower than for A_{WT}, but is nonexistent and similar to that seen in patches from H_2O-injected oocytes. These deviations from the whole-cell data may be due to different intracellular ion dependencies or sensitivities among the variants, and the fact that the macropatch experiments were performed with a symmetrical solution containing extracellular ion concentrations. High Na^+ and HCO_3^- concentrations on the cytosolic side were used to maximize the transporter currents. Another explanation is the involvement of cytosolic factors in the whole-cell experiments that are absent in the macropatch experiments. While such factors could either stimulate A or inhibit C, the $A_{\Delta N43}$ current observed in whole-cell but not macropatch experiments is consistent with a cytosolic factor stimulating the A variant.

Potential cytosolic factors include cytoskeletal elements such as actin or enzymes. Indeed, the amino-terminal domain of AE1 interacts with actin, protein 4.1, protein 4.2, as well as glycolytic enzymes (Reithmeier et al., 1996). Classic regulatory factors include cyclic AMP and ATP. Heyer et al. (1999) reported that 2 mM ATP increases the activity of rat NBCe1-A from inside-out macropatches by twofold. The effect of ATP on NBCe1 activity may be mediated by ATP-dependent lipid kinases and PIP_2, as previously reported for the cardiac Na-Ca exchanger and K_{ATP} potassium channels (Hilgemann and Ball, 1996). There is considerable evidence highlighting the regulatory effects of membrane phospholipids such as PIP_2 on ion channels and transporters (Suh and Hille, 2005). Future studies will be necessary to characterize potential regulatory factors such as ATP, PIP_2, and kinases/phosphatases that may differentially modulate the NBCe1 variants.

We thank Mr. Albert Tousson (High Resolution Imaging Center, University of Alabama at Birmingham) for assistance with confocal microscopy used in the immunocytochemical analysis of NBC expression in oocytes. Dr. Peter R. Smith (Physiology and Biophysics, University of Alabama at Birmingham) provided assistance and the luminometer used for single-oocyte chemiluminescence. A special thanks goes to Dr. Chou-Long Huang (University of Texas Southwestern Medical Center at Dallas, Dallas, TX) for providing guidance with the macropatch technique. We thank Mrs. Debeshi Majumdar for her helpful suggestions and comments regarding the manuscript.

This work was supported by the American Heart Association, Southeast Affiliate (0265083B) and National Institutes of Health/National Institute of Neurological Disorders and Stroke (NS046653).

Olaf S. Andersen served as editor.

Submitted: 15 February 2006
Accepted: 24 April 2006

REFERENCES

Abuladze, N., M. Song, A. Pushkin, D. Newman, I. Lee, S. Nicholas, and I. Kurtz. 2000. Structural organization of the human NBC1 gene: kNBC1 is transcribed from an alternative promoter in intron 3. *Gene.* 251:109–122.

Bevensee, M.O., M. Apkon, and W.F. Boron. 1997a. Intracellular pH regulation in cultured astrocytes from rat hippocampus. II. Electrogenic Na/HCO_3 cotransport. *J. Gen. Physiol.* 110:467–483.

Bevensee, M.O., R.A. Weed, and W.F. Boron. 1997b. Intracellular pH regulation in cultured astrocytes from rat hippocampus. I. Role of HCO_3^-. *J. Gen. Physiol.* 110:453–465.

Bevensee, M.O., B.M. Schmitt, I. Choi, M.F. Romero, and W.F. Boron. 2000. An electrogenic Na^+-HCO_3^- cotransporter (NBC) with a novel COOH-terminus, cloned from rat brain. *Am. J. Physiol. Cell Physiol.* 278:C1200–C1211.

Boron, W.F., and E.L. Boulpaep. 1983. Intracellular pH regulation in the renal proximal tubule of the salamander: basolateral HCO_3^- transport. *J. Gen. Physiol.* 81:53–94.

Boron, W.F., P. Fong, M.A. Hediger, E.L. Boulpaep, and M.F. Romero. 1997. The electrogenic Na/HCO_3 cotransporter. *Weiner Klin Wochenschr.* 109:445–456.

Chesler, M. 2003. Regulation and modulation of pH in the brain. *Physiol. Rev.* 83:1183–1221.

Choi, I., C. Aalkjaer, E.L. Boulpaep, and W.F. Boron. 2000. An electroneutral sodium/bicarbonate cotransporter NBCn1 and associated sodium channel. *Nature.* 405:571–575.

Choi, I., M.F. Romero, N. Khandoudi, A. Bril, and W.F. Boron. 1999. Cloning and characterization of a human electrogenic Na^+-HCO_3^- cotransporter isoform (hhNBC). *Am. J. Physiol.* 276:C576–C584.

Cordat, E., J. Li, and R.A. Reithmeier. 2003. Carboxyl-terminal truncations of human anion exchanger impair its trafficking to the plasma membrane. *Traffic.* 4:642–651.

Deitmer, J.W., and W.-R. Schlue. 1989. An inwardly directed electrogenic sodium-bicarbonate cotransport in leech glial cells. *J. Physiol.* 411:179–194.

Dinour, D., M.H. Chang, J. Satoh, B.L. Smith, N. Angle, A. Knecht, I. Serban, E.J. Holtzman, and M.F. Romero. 2004. A novel missense mutation in the sodium bicarbonate cotransporter (NBCe1/*SLC4A4*) causes proximal tubular acidosis and glaucoma through ion transport defects. *J. Biol. Chem.* 279:52238–52246.

Grichtchenko, I.I., M.F. Romero, and W.F. Boron. 2000. Extracellular HCO_3^- dependence of electrogenic Na/HCO_3 cotransporters cloned from salamander and rat kidney. *J. Gen. Physiol.* 115:533–546.

Gross, E., A. Pushkin, N. Abuladze, O. Fedotoff, and I. Kurtz. 2002. Regulation of the sodium bicarbonate cotransporter kNBC1 function: role of Asp(986), Asp(988) and kNBC1-carbonic anhydrase II binding. *J. Physiol.* 544:679–685.

Gross, E., O. Fedotoff, A. Pushkin, N. Abuladze, D. Newman, and I. Kurtz. 2003. Phosphorylation-induced modulation of pNBC1 function: distinct roles for the amino- and carboxy-termini. *J. Physiol.* 549:673–682.

Gross, E., K. Hawkins, N. Abuladze, A. Pushkin, C.U. Cotton, U. Hopfer, and I. Kurtz. 2001. The stoichiometry of the electrogenic sodium bicarbonate cotransporter NBC1 is cell-type dependent. *J. Physiol.* 531:597–603.

Gross, E., K. Hawkins, A. Pushkin, P. Sassani, R. Dukkipati, N. Abuladze, U. Hopfer, and I. Kurtz. 2001. Phosphorylation of Ser^{982} in the sodium bicarbonate cotransporter kNBC1 shifts the HCO_3^-:Na^+ stoichiometry from 3:1 to 2:1 in murine proximal tubule cells. *J. Physiol.* 537:659–665.

Heyer, M., S. Müller-Berger, M.F. Romero, W.F. Boron, and E. Frömter. 1999. Stoichiometry of the rat kidney Na^+-HCO_3^- cotransporter expressed in *Xenopus laevis* oocytes. *Pflugers Arch.* 438:322–329.

Hilgemann, D.W. 1995. The giant membrane patch. *In* Single Channel Recording. Second edition. B. Sackmann and E. Neher, editors. Plenum Press, New York. 307–327.

Hilgemann, D.W., and R. Ball. 1996. Regulation of cardiac Na^+, Ca^{2+} exchanger and K_{ATP} potassium channels by PIP_2. *Science.* 273:956–959.

Huang, C.L., S. Feng, and D.W. Hilgemann. 1998. Direct activation of inward rectifier potassium channels by PIP_2 and its stabilization by $G_{\beta\gamma}$. *Nature.* 391:803–806.

Igarashi, T., J. Inatomi, T. Sekine, S.H. Cha, Y. Kanai, M. Kunimi, K. Tsukamoto, H. Satoh, M. Shimadzu, F. Tozawa, et al. 1999. Mutations in *SLC4A4* cause permanent isolated proximal renal tubular acidosis with ocular abnormalities. *Nat. Genet.* 23:264–266.

Kozak, M. 1986. Point mutations define a sequence flanking the AUG initiator codon that modulates translation by eukaryotic ribosomes. *Cell.* 44:283–292.

Li, H.C., P. Szigligeti, R.T. Worrell, J.B. Matthews, L. Conforti, and M. Soleimani. 2005. Missense mutations in Na^+:HCO_3^- cotransporter NBC1 show abnormal trafficking in polarized kidney cells: a basis of proximal renal tubular acidosis. *Am. J. Physiol. Renal Physiol.* 289:F61–F71.

Li, H.C., R.T. Worrell, J.B. Matthews, H. Husseinzadeh, L. Neumeier, S. Petrovic, L. Conforti, and M. Soleimani. 2004. Identification of a carboxyl-terminal motif essential for the targeting of Na^+-HCO_3^- cotransporter NBC1 to the basolateral membrane. *J. Biol. Chem.* 279:43190–43197.

Machaca, K., Z. Qu, A. Kuruma, H.C. Hartzell, and N. McCarty. 2002. The endogenous calcium-activated Cl channel in *Xenopus* oocytes: a physiologically and biologically rich model system. *In* Current Topics in Membranes. Vol. 53. C.M. Fuller, editor. Academic Press, Amsterdam. 3–39.

Margeta-Mitrovic, M., Y.N. Jan, and L.Y. Jan. 2000. A trafficking checkpoint controls GABA(B) receptor heterodimerization. *Neuron.* 27:97–106.

McAlear, S.D., and M.O. Bevensee. 2004. pH regulation in non-neuronal brain cells and interstitial fluid. *In* Advances in Molecular and Cell Biology. Vol. 31. L. Hertz, editor. Elsevier, Amsterdam. 707–745.

McNicholas, C.M., W.-H. Wang, K. Ho, S.C. Hebert, and G. Giebisch. 1994. Regulation of ROMK1 K^+ channel activity involves phosphorylation processes. *Proc. Natl. Acad. Sci. USA.* 91:8077–8081.

Nelson, N., A. Sacher, and H. Nelson. 2002. The significance of molecular slips in transport systems. *Nat. Rev. Mol. Cell Biol.* 3:876–881.

O'Connor, E.R., H. Sontheimer, and B.R. Ransom. 1994. Rat hippocampal astrocytes exhibit elecrogenic sodium-bicarbonate co-transport. *J. Neurophysiol.* 72:2580–2589.

Reithmeier, R.A.F., S.L. Chan, and M. Popov. 1996. Structure of the erythrocyte Band 3 anion exchanger. *In* Handbook of Biological Physics. W.N. Konings., H.R. Kaback, and J.S. Lolkema, editors. Elsevier Science, Amsterdam. 281–309.

Romero, M.F., C.M. Fulton, and W.F. Boron. 2004. The *SLC4* family of HCO_3^- transporters. *Pflugers Arch.* 447:495–509.

Romero, M.F., M.A. Hediger, E.L. Boulpaep, and W.F. Boron. 1997. Expression cloning and characterization of a renal electrogenic Na^+/HCO_3^- cotransporter. *Nature.* 387:409–413.

Romero, M.F., Y. Kanai, H. Gunshin, and M.A. Hediger. 1998a. Expression cloning using *Xenopus laevis* oocytes. *Methods Enzymol.* 296:17–52.

Romero, M.F., P. Fong, U.V. Berger, M.A. Hediger, and W.F. Boron. 1998b. Cloning and functional expression of rNBC, an electrogenic Na^+-HCO_3^- cotransporter from rat kidney. *Am. J. Physiol.* 274:F425–F432.

Schmitt, B.M., D. Biemesderfer, M.F. Romero, E.L. Boulpaep, and W.F. Boron. 1999. Immunolocalization of the electrogenic Na^+-HCO_3^- cotransporter in mammalian and amphibian kidney. *Am. J. Physiol.* 276:F27–F36.

Sciortino, C.M., and M.F. Romero. 1999. Cation and voltage dependence of rat kidney electrogenic Na^+-HCO_3^- cotransporter, rkNBC, expressed in oocytes. *Am. J. Physiol.* 277:F611–F623.

Soleimani, M., S.M. Grassl, and P.S. Aronson. 1987. Stoichiometry of Na^+-HCO_3^- cotransport in basolateral membrane vesicles isolated from rabbit renal cortex. *J. Clin. Invest.* 79:1276–1280.

Suh, B.C., and B. Hille. 2005. Regulation of ion channels by phosphatidylinositol 4,5-bisphosphate. *Curr. Opin. Neurobiol.* 15:370–378.

Taylor, A.M., Q. Zhu, and J.R. Casey. 2001. Cystein-directed cross-linking localizes regions of the human erythrocyte anion-exchange protein (AE1) relative to the dimeric interface. *Biochem. J.* 359:661–668.

Tseng-Crank, J., J.A. Yao, M.F. Berman, and G.N. Tseng. 1993. Functional role of the NH_2-terminal cytoplasmic domain of a mammalian A-type K channel. *J. Gen. Physiol.* 102:1057–1083.

Virkki, L.V., D.A. Wilson, R.D. Vaughan-Jones, and W.F. Boron. 2002. Functional characterization of human NBC4 as an electrogenic Na^+-HCO_3^- cotransporter (NBCe2). *Am. J. Physiol. Cell Physiol.* 282:C1278–C1289.

Weber, W.-M. 2002. Ca^{2+}-inactivated Cl^- channels in *Xenopus laevis* oocytes. *In* Current Topics in Membranes. Vol. 53. C.M. Fuller, editor. Academic Press, Amsterdam. 41–55.

Yoo, D., B.Y. Kim, C. Campo, L. Nance, A. King, D. Maouyo, and P.A. Welling. 2003. Cell surface expression of the ROMK (Kir 1.1) channel is regulated by the aldosterone-induced kinase, SGK-1, and protein kinase A. *J. Biol. Chem.* 278:23066–23075.

Zagotta, W.N., T. Hoshi, and R.W. Aldrich. 1990. Restoration of inactivation in mutants of Shaker potassium channels by a peptide derived from ShB. *Science.* 250:568–571.

Zerangue, N., B. Schwappach, Y.N. Jan, and L.Y. Jan. 1999. A new ER trafficking signal regulates the subunit stoichiometry of plasma membrane K_{ATP} channels. *Neuron.* 22:537–548.